Electronic Supplementary Information

Lithium halide ion-pair recognition mediated molecular shuttling in heteroditopic [2]rotaxanes

Vihanga Munasinghe[a‡], Hui Min Tay[a‡], Dilhan Manawadu[b], Jessica Pancholi[a], Zongyao Zhang[a] and Paul Beer[a]*
[a]Department of Chemistry, University of Oxford, South Parks Road, Oxford, OX1 3TA, UK.
[b]Department of Chemistry, University of Oxford, Physical and Theoretical Chemistry Laboratory, Oxford OX13QZ (UK)
E-mail: paul.beer@chem.ox.ac.uk

Table of Contents

S1. Synthesis of compounds 2
S1.1. General Information 2
S1.2. Synthetic procedures and characterisation 2
Synthesis of macrocycle **6** 2
Synthesis of rotaxanes **9** and **10** 6
S1.3. Spectral characterisation of novel precursors 9
S2. Solid State Structures 25
S3. ^{1}H NMR binding studies 27
S3.1. General Procedure 27
^{1}H NMR titrations of rotaxane **9** 28
^{1}H NMR titrations of Rotaxane **10** 34
^{1}H NMR titrations of macrocycle **6** 39
S3.2. Cation binding studies with Rotaxane 9 41
S4. DFT calculations 43
S4.1. DFT optimised structures 44
S4.2. Electrostatic potential map 48
S5. References 49

S1. Synthesis of compounds

S1.1. General Information

All solvents and reagents were purchased from commercial suppliers and used as received unless otherwise stated. Dry solvents were obtained by purging with nitrogen and then passing through an MBraun MPSP-800 column. H_2O was de-ionized and micro filtered using a Milli-Q® Millipore machine. Column chromatography was carried out on Merck® silica gel 60 under a positive pressure of nitrogen. Routine NMR spectra were recorded on either a Varian Mercury 300, a Bruker AVIII 400 or a Bruker AVIII 500 spectrometer with ^{1}H NMR titrations recorded on a Bruker AVIII 500 spectrometer. TBA salts were stored in a vacuum desiccator containing phosphorus pentoxide prior to use. Where mixtures of solvents were used, ratios are reported by volume. Chemical shifts are quoted in parts per million relative to the residual solvent peak. Mass spectra were recorded on a Bruker μTOF spectrometer.

S1.2. Synthetic procedures and characterisation

Synthesis of macrocycle **6**

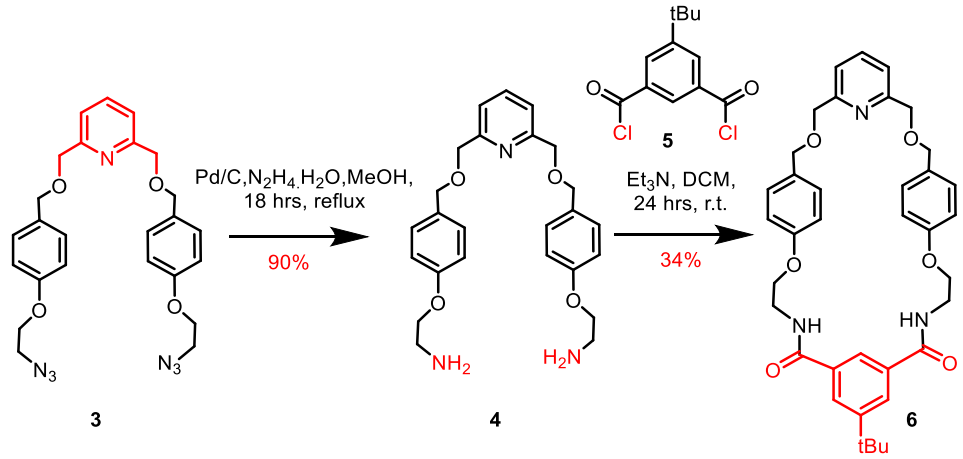

*Scheme S1.1 Synthesis of macrocycle **6***

Compound **3**[1] and **5**[2] were synthesized according to literature procedures.

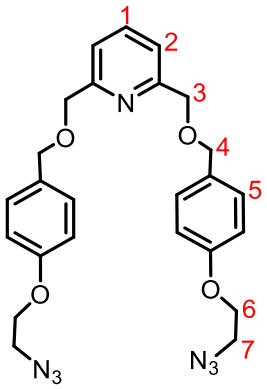

3

Compound 3: The alcohol precursor **1** (1.50g,7.76 mmol) was dissolved in 50 ml of dry THF. NaH (0.295 g of a 60% dispersion in mineral oil, 7.37 mmol) was added to the reaction mixture and was stirred at room temperature under N_2 for 20 minutes. Subsequently, the bis bromo pyridine precursor **2** was added and was stirred for a further 60 mins and then was heated at 50 °C for 48 hours. Solvent was then removed *in vacuo*. The residue was redissolved in DCM (50 ml), washed with brine (50 ml x 2), dried over $MgSO_4$ and solvent was removed *in vacuo*. The crude product was purified by silica gel column chromatography (0-2% MeOH in DCM) to afford the macrocycle precursor **3** as a white solid (1.14 g, 70%).

^{1}H NMR (500 MHz, $CDCl_3$) δ 7.58 (t, *J* = 7.7 Hz, 1H, H_1), 7.27 (d, *J* = 7.7 Hz, 2H, H_2), 7.20 (d, *J* = 8.5 Hz, 4H, H_4), 6.78 (d, *J* = 8.5 Hz, 4H, H_3), 4.53 (s, 4H, H_5), 4.46 (s, 4H, H_5), 3.99 (t, *J* = 5.0 Hz, 4H, H_6), 3.43 (t, *J* = 5.0 Hz, 4H, H_7)

^{13}C NMR (126 MHz, $CDCl_3$) δ 157.87, 137.15, 130.79, 129.43, 119.91, 114.46, 72.79, 72.39, 66.91, 50.02.

HRMS (ESI +ve) m/z: 490.2197 ($[M+H]^+$, $C_{25}H_{28}N_7O_4$ requires 490.2197)

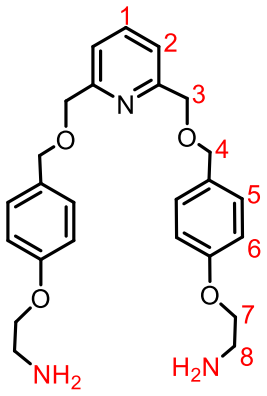

4

Compound 4: To a bis-azide precursor **3** (2.23 g, 4.55 mmol) in methanol, 10% Pd/C (0.25 g) and hydrazine monohydrate (2.21 mL, 2.28 g, 45.5 mol) were added and the reaction mixture was refluxed under N_2 for 18 hours. Reaction mixture was cooled to room temperature and was filtered through a plug of Celite. Filtrate was collected and solvent evaporated *in vacuo* to afford the bis-amine precursor **4** as a white solid (1.79 g, 90%).

^{1}H NMR (400 MHz, $CDCl_3$) δ 7.69 (t, *J* = 7.7 Hz, 1H, H_1), 7.37 (d, *J* = 7.7 Hz, 2H, H_2), 7.29 (d, *J* = 8.5 Hz, 4H, H_6), 6.82 (d, *J* = 8.5 Hz, 4H, H_5), 4.63 (s, 4H, H_3), 4.56 (s, 4H, H_4), 3.98 (t, *J* = 5.2 Hz, 4H, H_8), 3.07 (t, *J* = 5.2 Hz, 4H, H_7),

^{13}C NMR (101 MHz, $CDCl_3$) δ 158.75, 158.10, 137.34, 130.38, 129.62, 120.08, 114.57, 72.92, 72.69, 70.32, 41.69

HRMS (ESI +ve): 438.2386 $[M+H]^+$ ($[C_{25}H_{32}N_3O_4]^+$ calc. 438.2387)

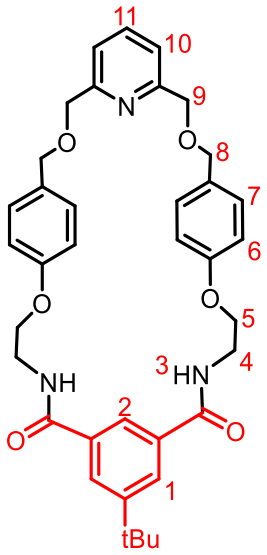

6

Macrocycle 6: 5-tert-Butylisophthalic acid was suspended in dry DCM (15 mL). Oxalyl chloride (0.34 mL, 0.51 g, 4.02 mmol) and DMF (2 drops) were added and the reaction mixture and was stirred under N_2 at room temperature until a homogenous solution was observed. Solvent was evaporated *in vacuo.* The resultant solid was redissolved in dry DCM (15 mL) and was added dropwise to a solution of the macrocyclic precursor **5** (0.438 g, 1.0 mmol) and Et_3N (0.7 mL, 5 mmol) in dry DCM. Reaction mixture was stirred overnight at room temperature under N_2 atmosphere. The resultant mixture was washed with 10% $HCl_{(aq)}$, sat. $NaHCO_3$ and brine and dried over $MgSO_4$ and solvent evaporated *in vacuo* to afford macrocycle **6** as a white solid (0.212 g, 34%).

^{1}H NMR (500 MHz, Chloroform-*d*) δ 7.97 (s, 2H, H_1), 7.92 (s, 1H, H_2), 7.68 (t, *J* = 7.7 Hz, 1H, H_{11}), 7.32 (d, *J* = 7.7 Hz, 2H, H_{10}), 7.21 (d, J= 7.7, 4H, H_6), 6.85 (t, *J* = 5.9 Hz, 2H, H_3), 6.79 (d, *J* = 7.7, 4H, H_7), 4.56 (s, 4H, H_9), 4.40 (s, 4H, H_8), 4.11 (t, *J* = 4.9 Hz, 4H, H_4), 3.90-3.84 (m, 4H, H_5), 1.26 (s, 9H, tBu).

^{13}C NMR (126 MHz, $CDCl_3$) δ 167.52, 158.27, 157.79, 152.82, 137.27, 134.53, 130.35, 130.21, 127.91, 121.85, 120.33, 114.44, 72.11, 71.40, 66.91, 39.75, 35.16, 31.25, 29.85.

HRMS (ESI +ve): 624.3062 $[M+H]^+$ ($[C_{37}H_{42}N_3O_6]^+$ calc. 624.3068)

Synthesis of rotaxanes **9** and **10**

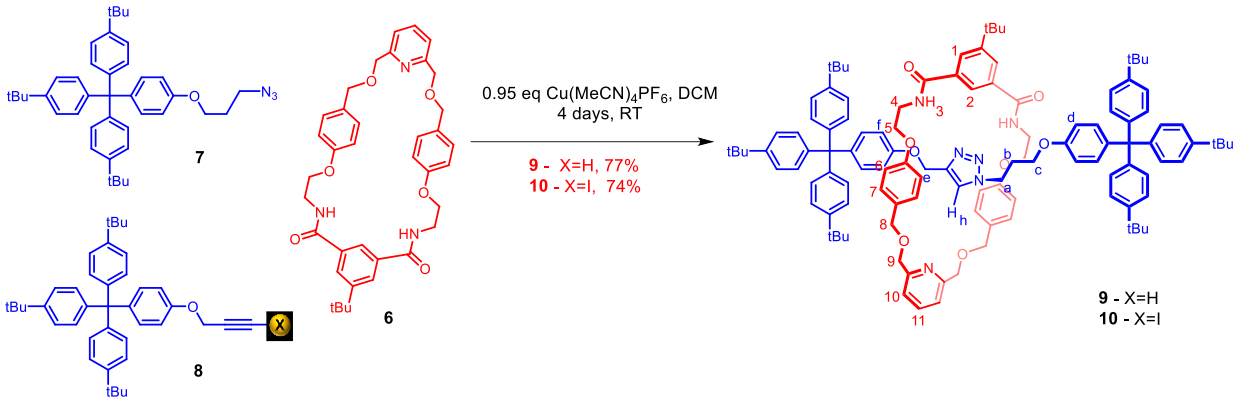

*Scheme S1.2: Synthesis of Rotaxanes **9** and **10.***

Axle precursors **7**[3] and **8**[4, 5] were synthesised according to literature procedures.

Rotaxane 9

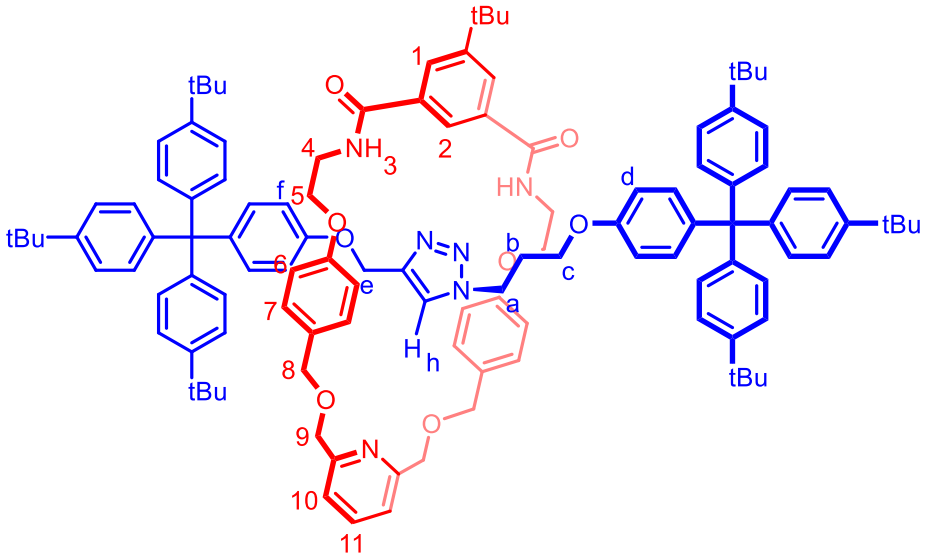

Rotaxane 9: Macrocycle **6** (8.0 mg, 0.012 mmol) and $[CuPF_6(MeCN)_4]$ (4.54 mg, 0.95 mmol) were dissolved in 0.6 ml dry degassed DCM and was stirred for 30 minutes. A solution of stopper azide **7** (30.1 mg, 0.05 mmol) and stopper alkyne **8** (27.8 mg, 0.05 mmol) in dry degassed DCM (0.6 ml) was added to the Cu-complexed macrocycle solution. The reaction mixture was sealed and the homogenous solution was stirred for 48 hours. Subsequently, the reaction mixture was diluted with 10 ml DCM, washed with basic EDTA/$NH_4OH_{(aq)}$ (10 ml x 3) and H_2O (10 ml x 2), dried over $MgSO_4$ and was concentrated in a rotary evaporator. The crude product was purified by preparative thin layer chromatography (SiO_2, 0-3% MeOH in DCM) to yield the desired rotaxane as a white solid (17.4 mg, 77%).

^{1}H NMR (500 MHz, $CDCl_3$) δ 8.29 (s, 1H, H_2), 8.24 (s, 2H, H_1), 7.51-7.59 (m, 3H, H_3,H_9), 7.24-7.30 (m, 15H, H_{10}, H_h, $H_{stopper\ ArH}$), 7.14 – 7.07 (m, 16H, $H_{stopper\ ArH}$), 7.03 (d, *J* = 8.1 Hz, 4H,H_7), 6.67 (d, *J* = 8.8 Hz, 2H, H_f), 6.61 (d, *J* = 8.8 Hz, 2H, H_d), 6.47 (d, *J* = 8.1 Hz, 4H, H_6), 4.77 (s, 2H,H_e), 4.45-4.55 (m, 4H, H_8), 4.41 – 4.33 (m, 4H, H_9), 3.86-3.97 (m, 4H, H_5), 3.62-3.79 (m, 6H, H_a,H_4), 3.51 (t, *J* = 5.7 Hz, 2H, H_c), 1.69 – 1.63 (m, 2H, H_b), 1.38-1.34 (m, 63H, $H_{t\text{-}Bu}$).

^{13}C NMR (126 MHz, $CDCl_3$) δ 167.80, 157.94, 157.50, 156.23, 155.92, 152.55, 148.48, 144.22, 144.12, 140.61, 140.21, 137.42, 134.04, 132.48, 132.35, 129.97, 128.99, 124.23, 121.31, 120.97, 114.35, 113.09, 113.02, 72.41, 71.82, 66.30, 63.96, 63.19, 61.19, 47.14, 39.71, 35.20, 34.43, 31.51, 31.36, 29.12.

HRMS: (ESI +ve) m/z: 1755.0437 ($[M+H]^+$, $C_{117}H_{137}N_6O_8$ requires 1755.0525)

Rotaxane 10

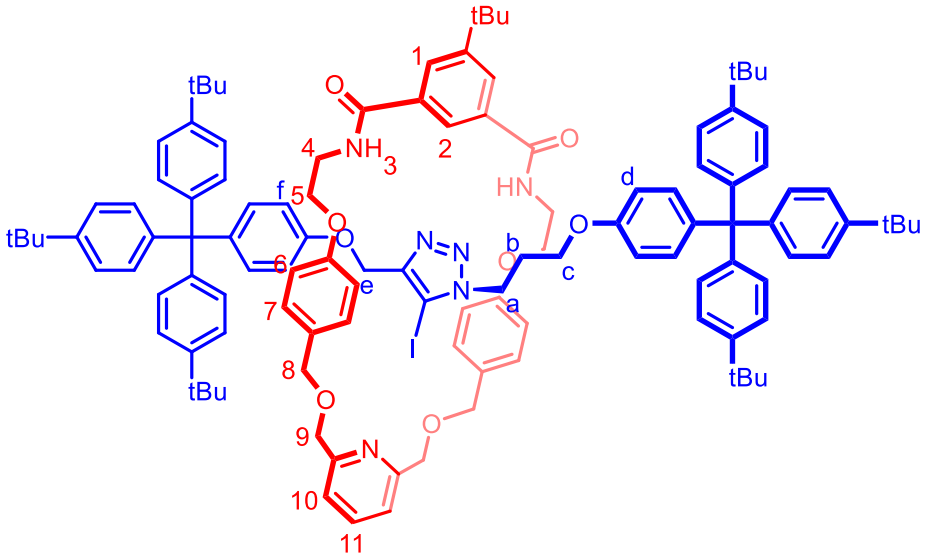

Rotaxane 10: Rotaxane **10** was synthesized following the same procedure used to synthesize rotaxane **9**, using the macrocycle **6** (10.0 mg, 0.016 mmol), [$CuPF_6(MeCN)_4$] (5.66 mg, 0.0095 mmol), stopper azide **7** (49.9 mg, 0.08 mmol), stopper alkyne **8** (53.5 mg, 0.08 mmol) in dry degassed DCM (1.6 ml total volume). The crude mixture was purified by preparative thin layer chromatography (SiO_2, 0-3% MeOH in DCM) to yield the desired rotaxane as a white solid (22.2 mg, 74%).

^{1}H NMR (500 MHz, $CDCl_3$) δ 8.58 (s, 1H, H_2), 8.23 (s, 2H,H_1), 7.63 (t, *J* = 7.7 Hz, 1H, H_{11}), 7.50 (t, *J* = 5.0 Hz, 2H, H_3), 7.32 (d, *J* = 7.8 Hz, 2H, H_{10}), 7.19-7.24 (m, 12H, $H_{stopper\ ArH}$), 7.04-7.12 (m, 20H, H_7,$H_{stopper\ ArH}$), 6.72 (d, *J* = 8.3 Hz, 2H, H_f), 6.65 (d, *J* = 8.4 Hz, 2H, H_d), 6.40 (d, *J* = 8.0 Hz, 4H, H_6), 4.78 (s, 2H, H_e), 4.56 – 4.46 (m, 4H, H_8), 4.46 – 4.34 (m, 4H, H_9), 3.95 (t, *J* = 7.6 Hz, 2H,H_a), 3.75 (t, *J* = 5.7 Hz, 2H, H_c), 3.49-3.58 (m, *J* = 5.0 Hz, 4H,H_4), 3.60 – 3.48 (m, 4H,H_5), 2.02 – 1.91 (m, 2H, H_b), 1.24-1.34 (m, 63H, $H_{t\text{-}Bu}$).

^{13}C NMR (126 MHz, $CDCl_3$) δ 167.73, 158.38, 157.31, 156.33, 152.54, 148.49, 144.21, 144.11, 140.79, 140.29, 137.72, 133.87, 132.46, 132.43, 130.82, 129.98, 129.07, 124.25, 122.00, 121.61, 114.32, 113.34, 113.07, 72.79, 71.85, 66.41, 64.10, 63.20, 61.47, 48.06, 40.28, 35.21, 34.43, 31.52, 31.38, 29.03.

HRMS: (ESI +ve) m/z: 940.9778 ($[M+2H]^{2+}$, $C_{117}H_{137}N_6O_8$ requires 940.9783)

S1.3. Spectral characterisation of novel precursors

Compound **4**

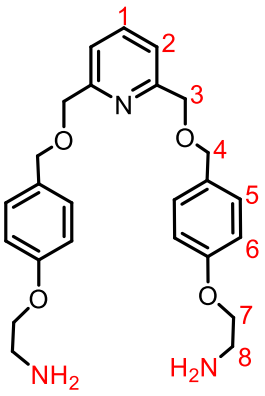

4

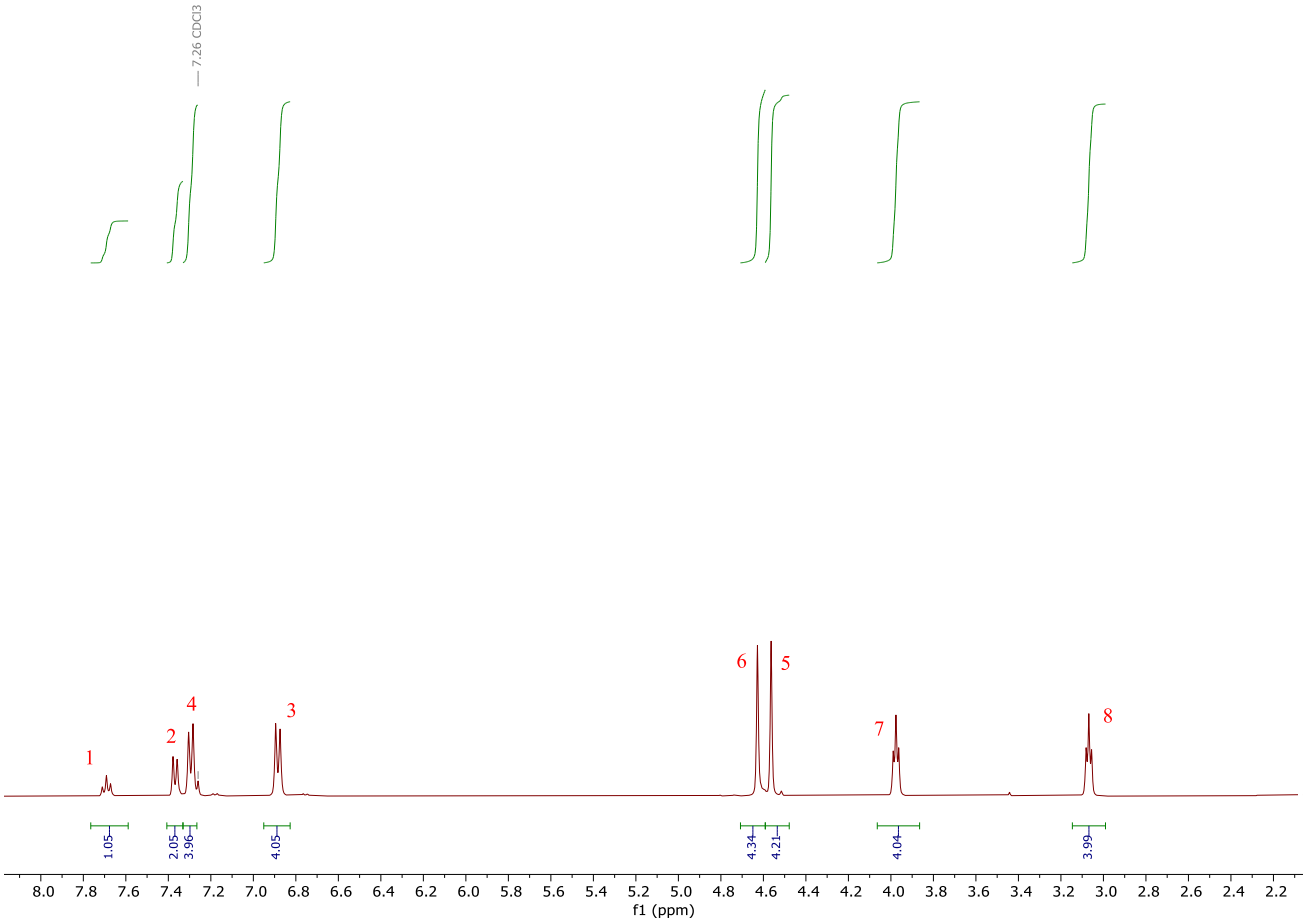

*Figure S1.1: ^{1}H NMR spectrum of macrocycle precursor **4** (500 MHz, 298 K, $CDCl_3$).*

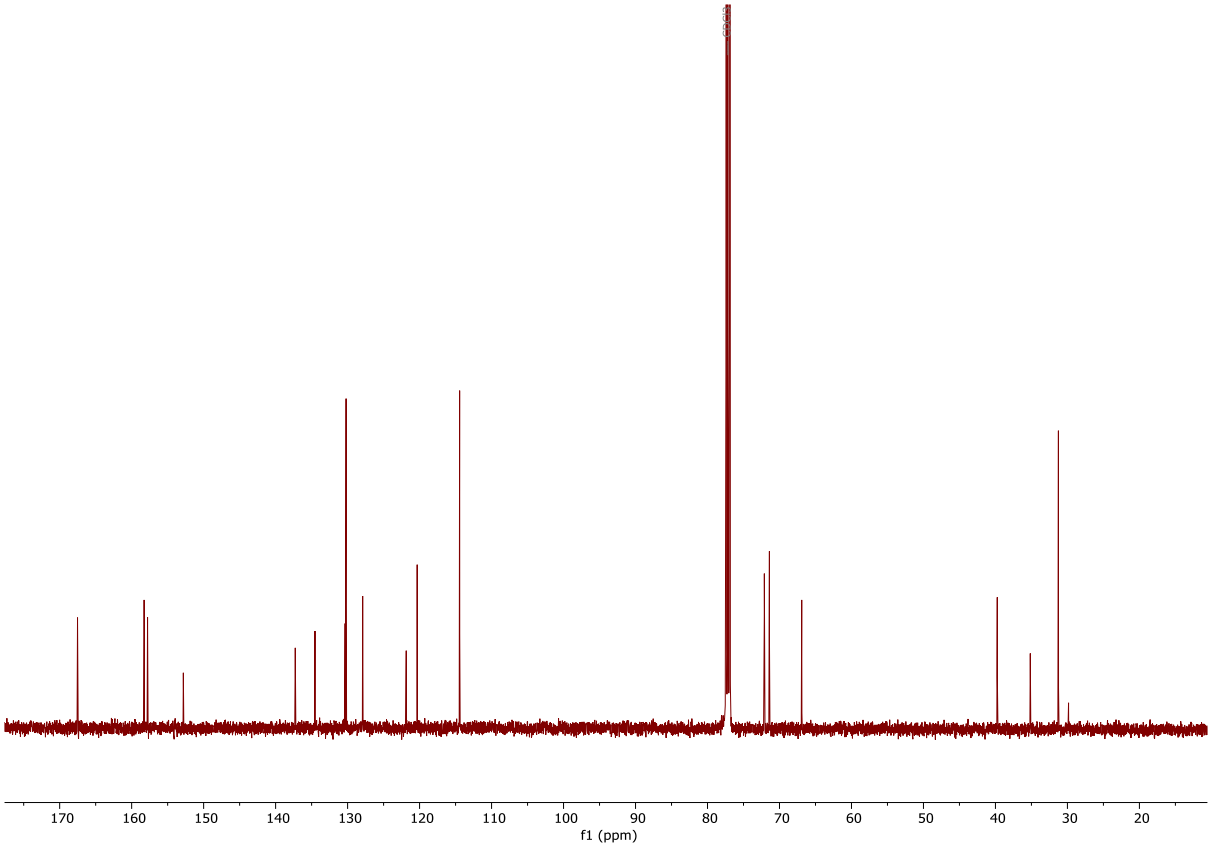

*Figure S1.2: : ^{13}C NMR spectrum of macrocycle precursor **4** (101 MHz, 298 K, $CDCl_3$).*

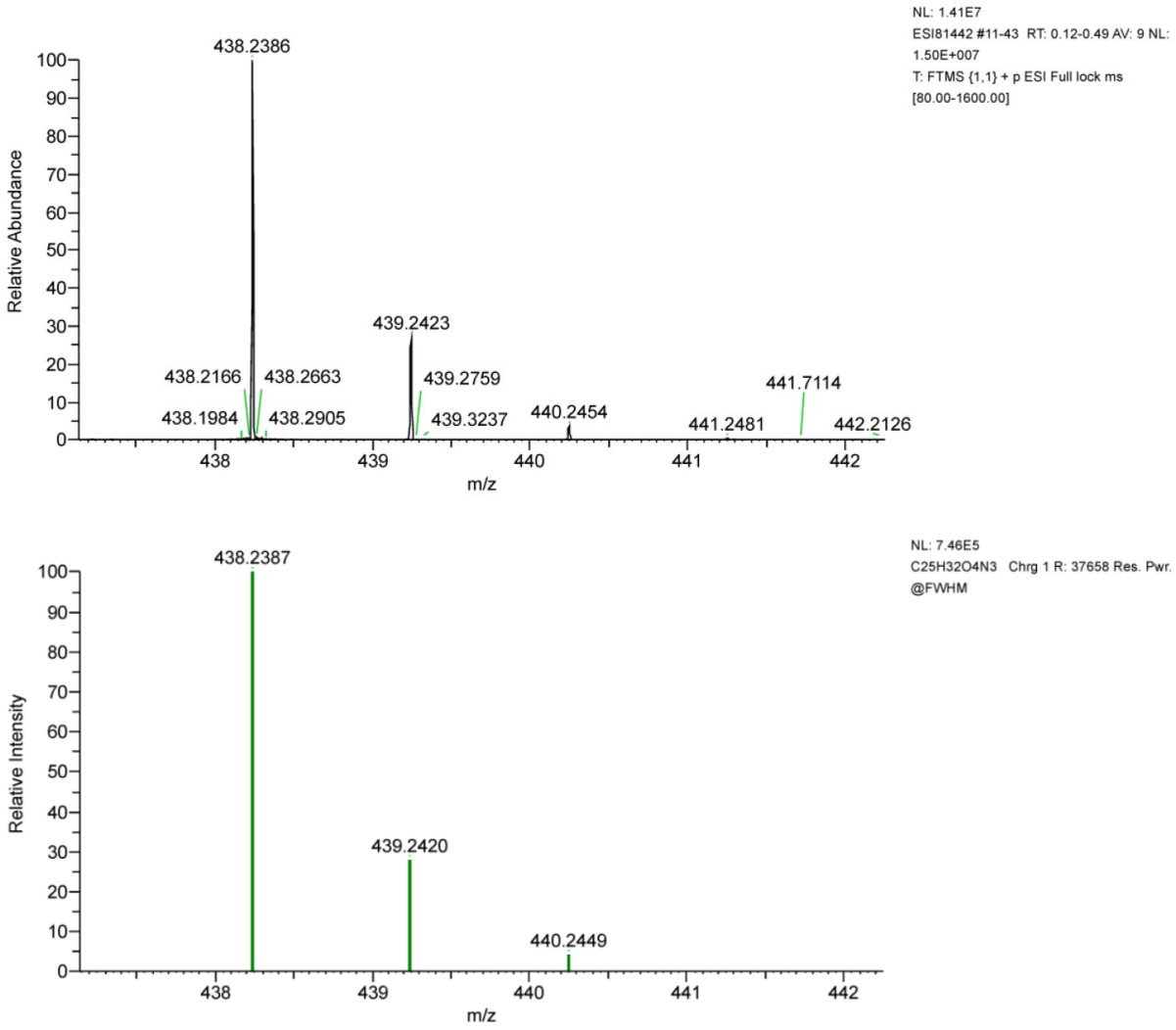

*Figure S1.3: High resolution ESI mass spectrum of macrocycle precursor **4** (top) and its theoretical spectrum (bottom)*

Macrocycle **6**

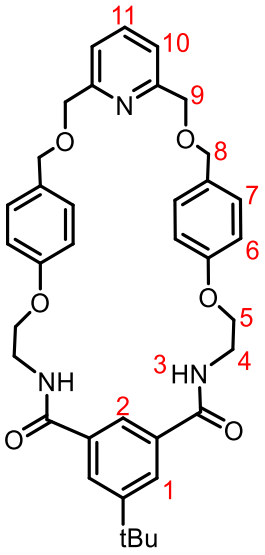

6

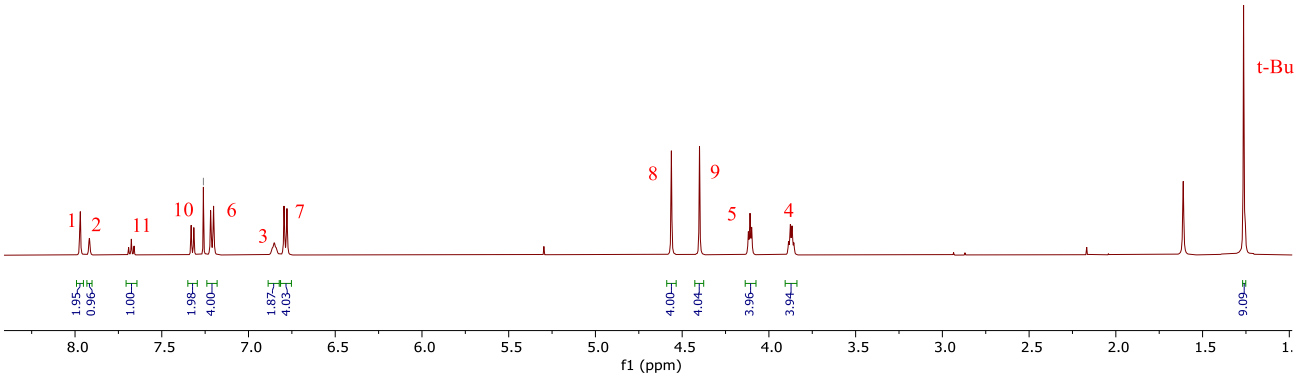

*Figure S1.4: ^{1}H NMR spectrum of macrocycle **6** (500 MHz, 298 K, $CDCl_3$)*

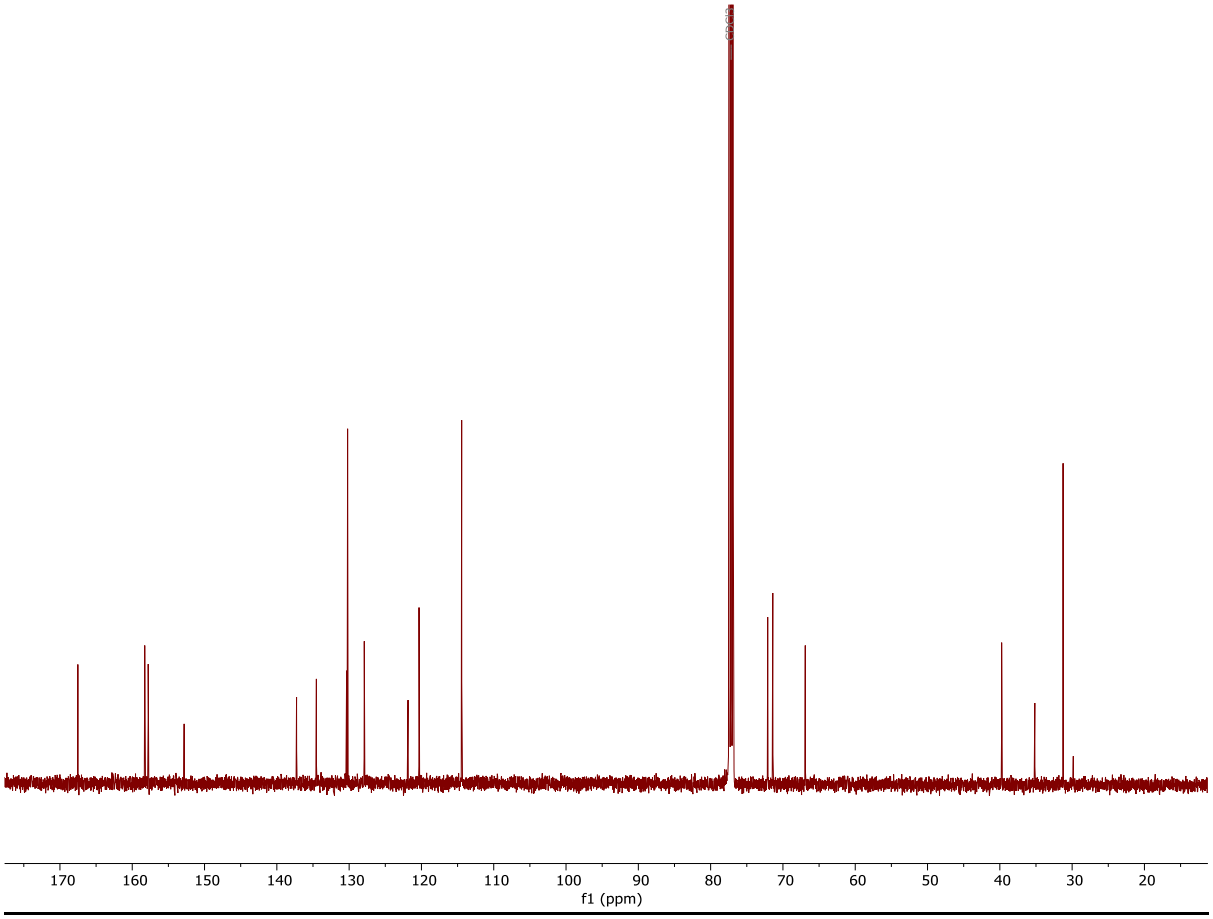

*Figure S1.5: ^{13}C NMR spectrum of macrocycle **6** (126 MHz, 298 K, $CDCl_3$).*

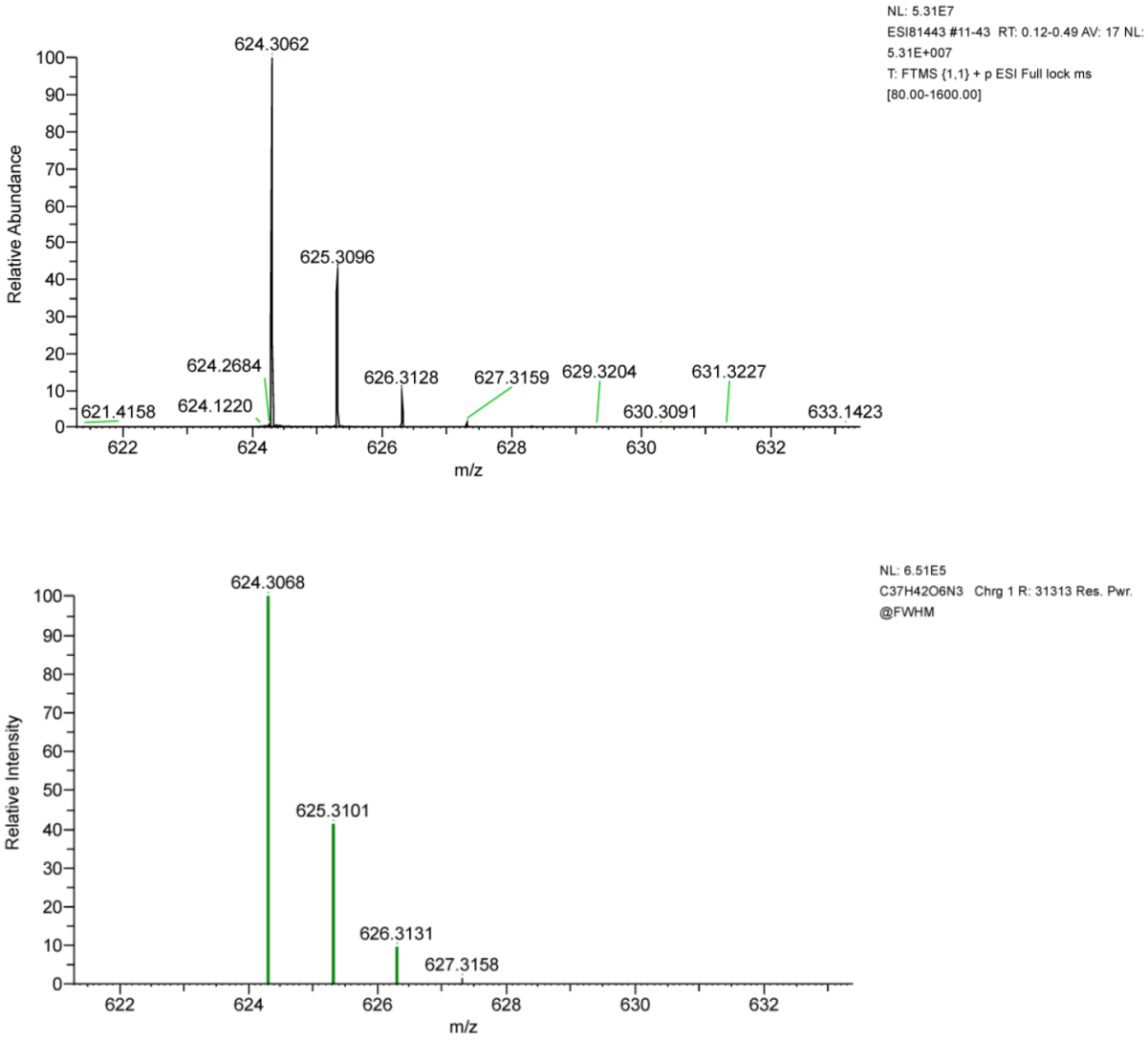

*Figure S1.6: High resolution ESI mass spectrum of macrocycle **6** (top) and its theoretical spectrum (bottom)*

Rotaxane **9**

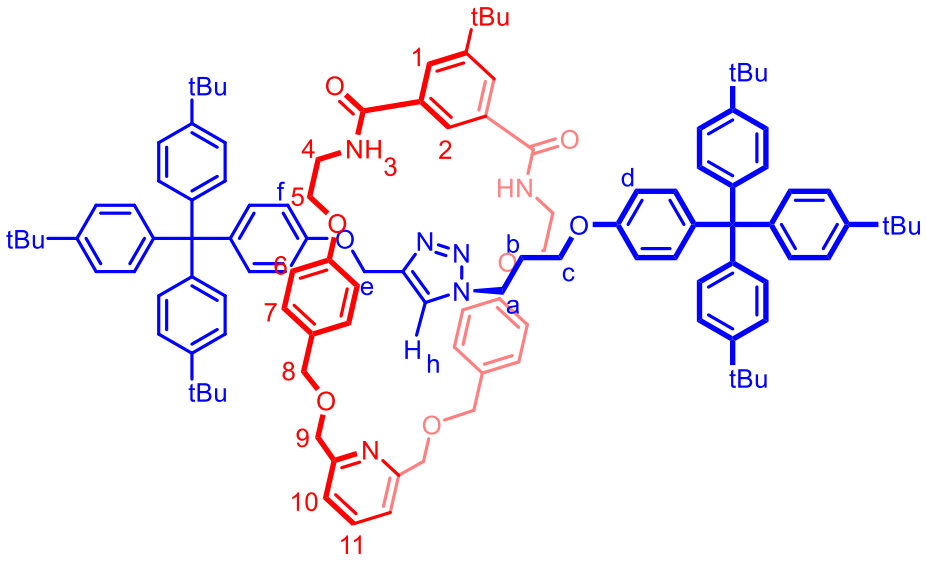

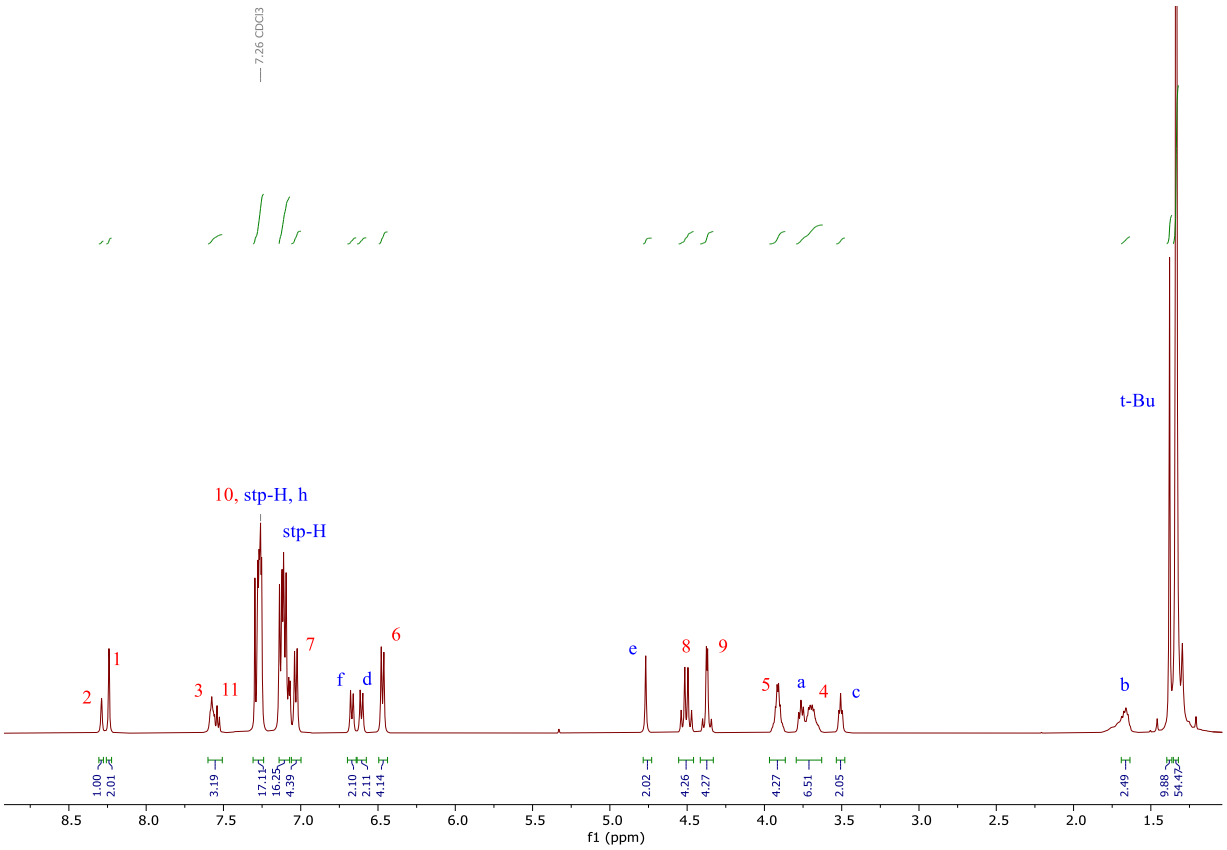

*Figure S1.7: ^{1}H NMR spectrum of Rotaxane **9** (500 MHz, 298 K, $CDCl_3$).*

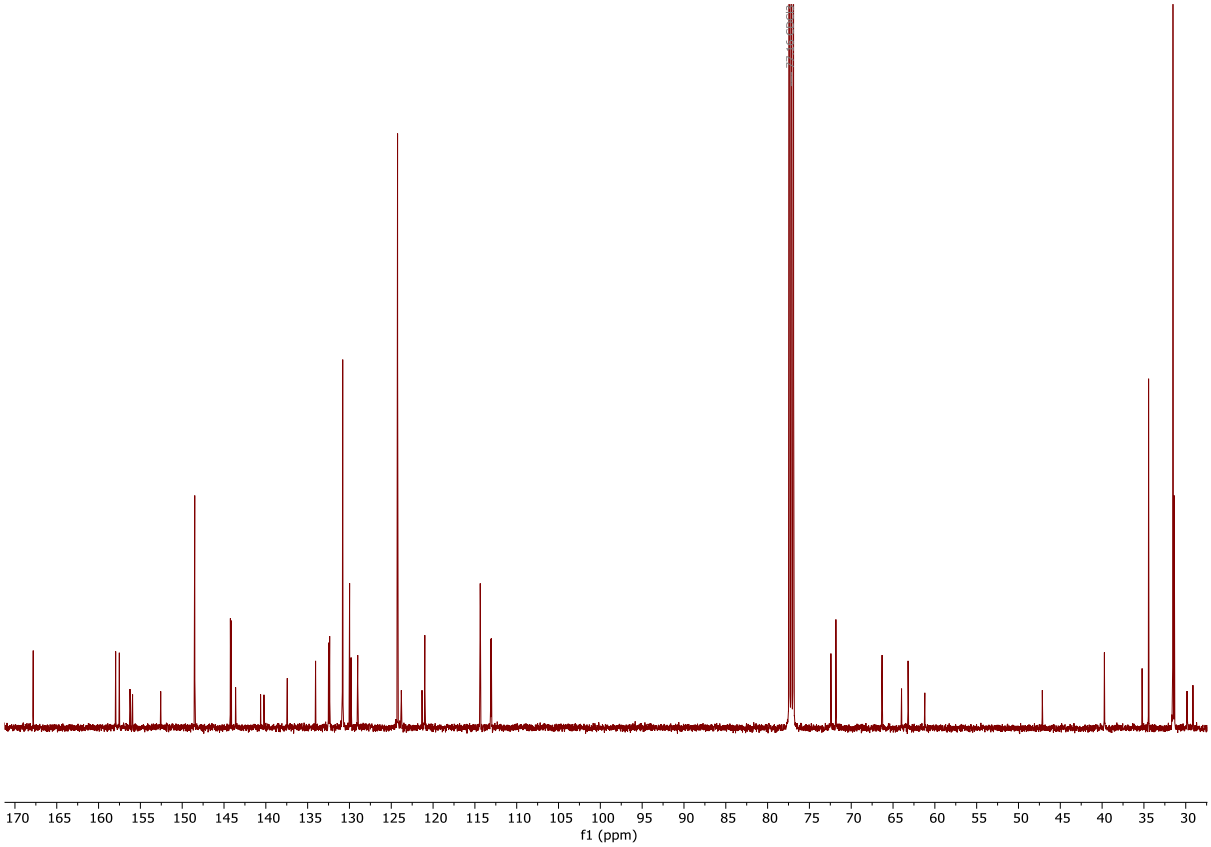

*Figure S1.8: ^{13}C NMR spectrum of Rotaxane **9** (126 MHz, 298 K, $CDCl_3$).*

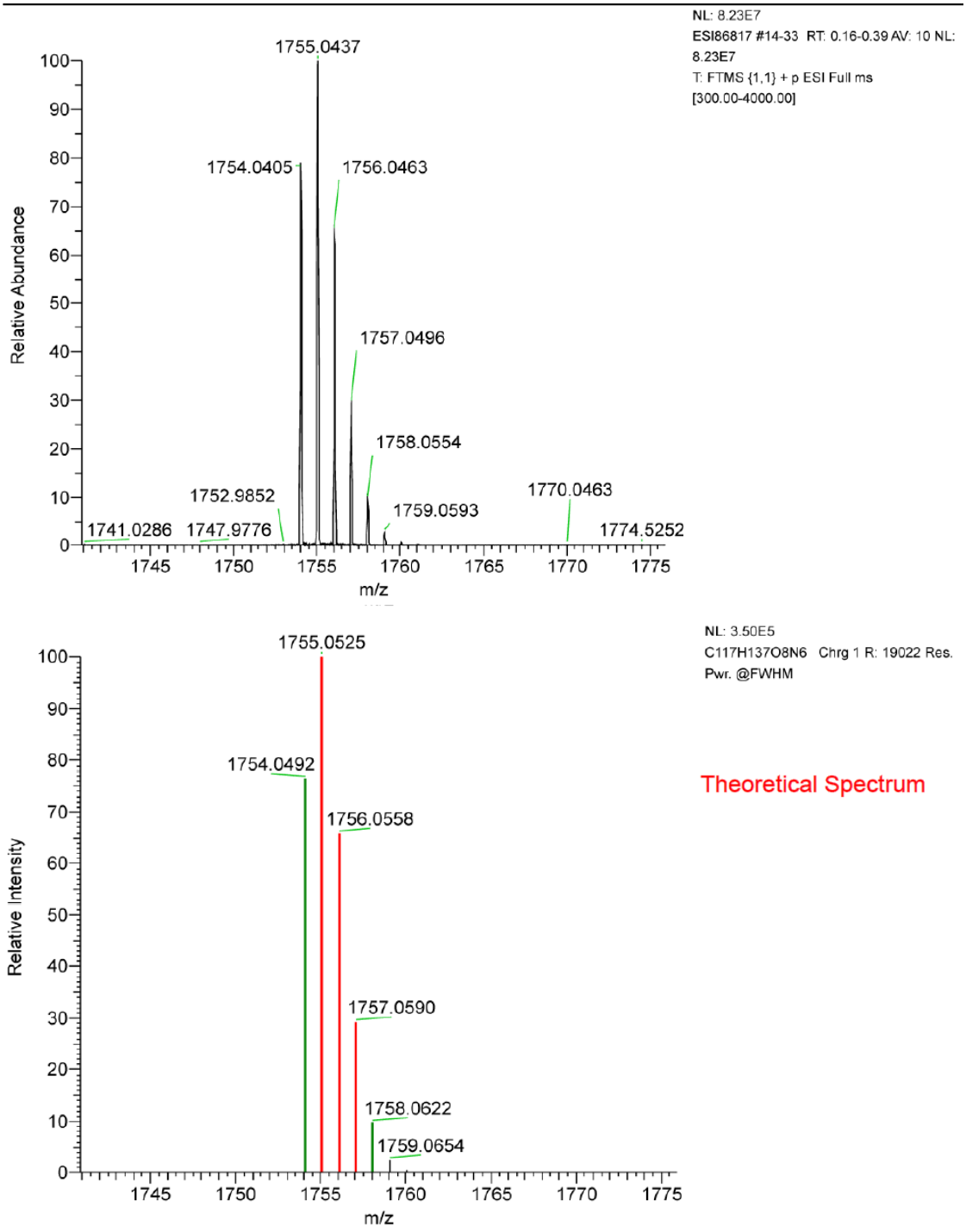

*Figure S1.9: High resolution ESI mass spectrum of Rotaxane **9** (top) and its theoretical spectrum (bottom)*

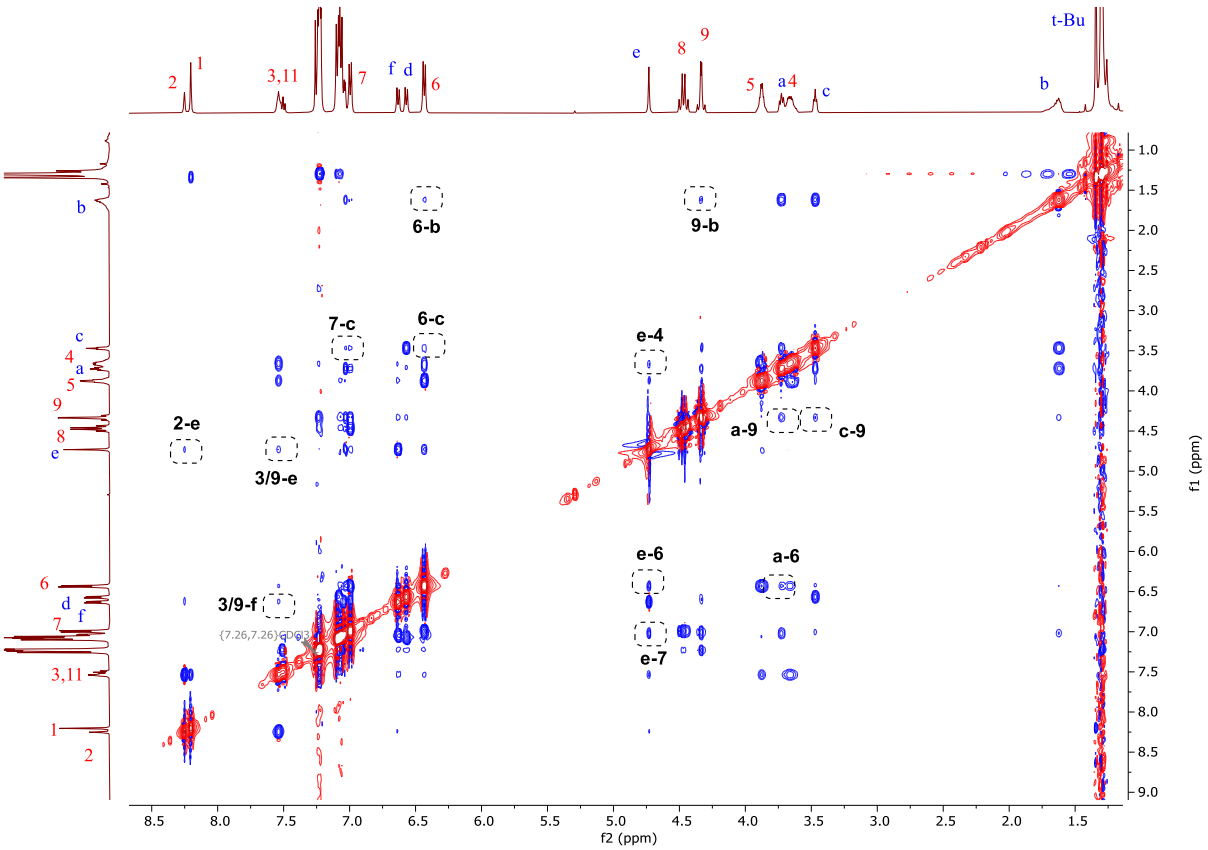

*Figure S1.10: ^{1}H-^{1}H ROESY NMR spectrum of the Rotaxane **9** ($CDCl_3$, 500 MHz, 298 K). Selected cross-peaks arising from through-space interactions of the interlocked macrocycle and axle components of the rotaxane are circled.*

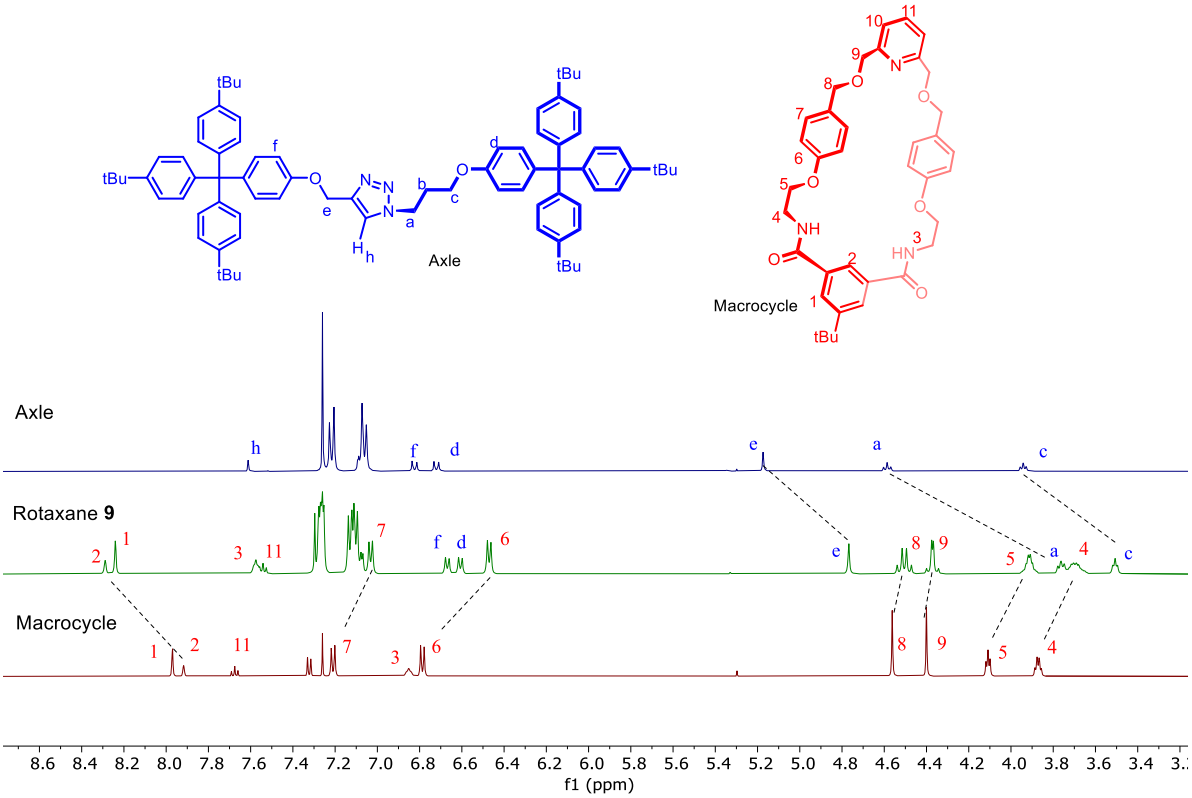

*Figure 1.11:Comparison of ^{1}H NMR spectra of axle (top), rotaxane **9** (middle) and macrocycle (bottom) ($CDCl_3$, 500 MHz, 298 K)*

Rotaxane **10**

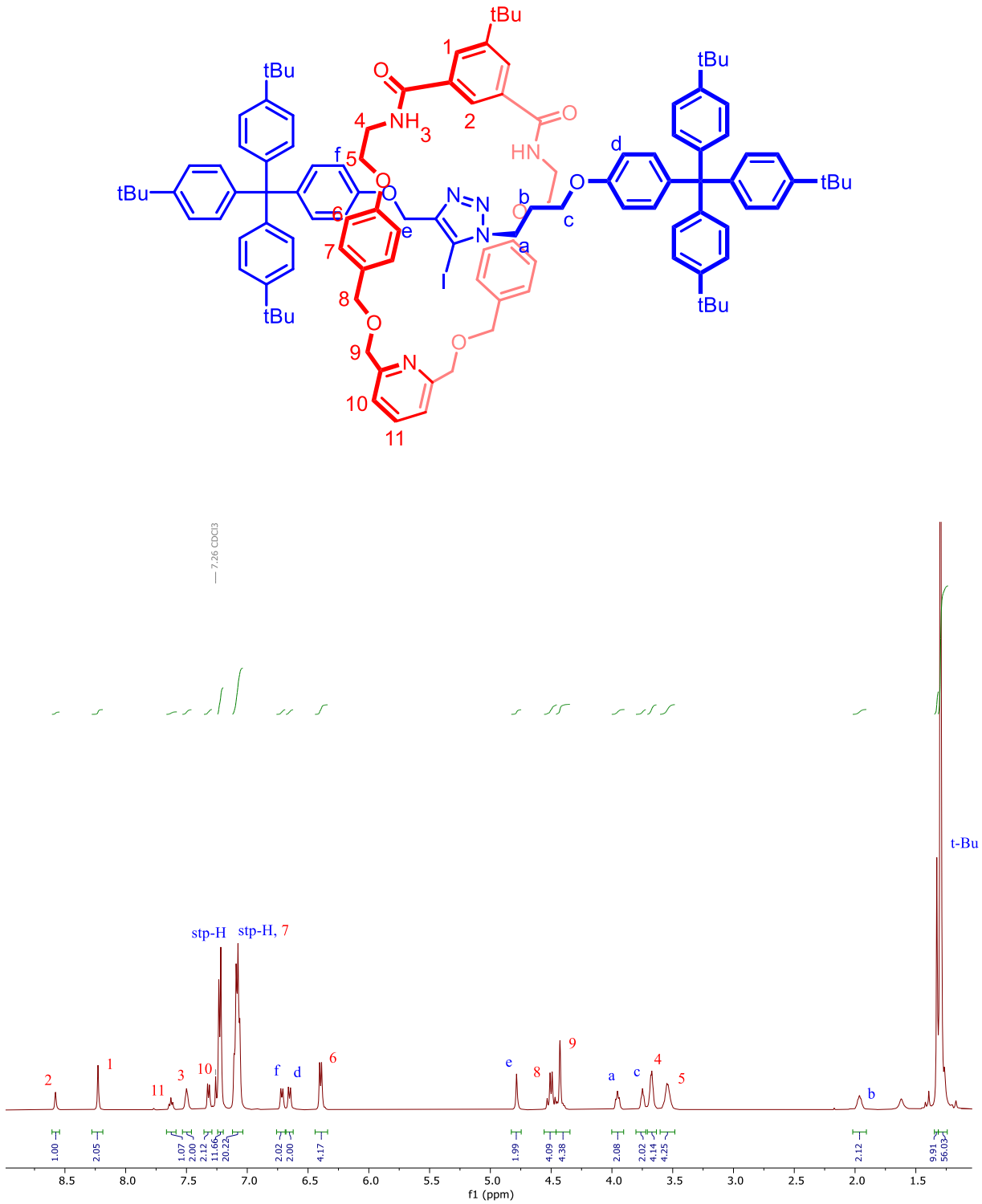

*Figure S1.12: ^{1}H NMR spectrum of Rotaxane **10** (400 MHz, 298 K, $CDCl_3$).*

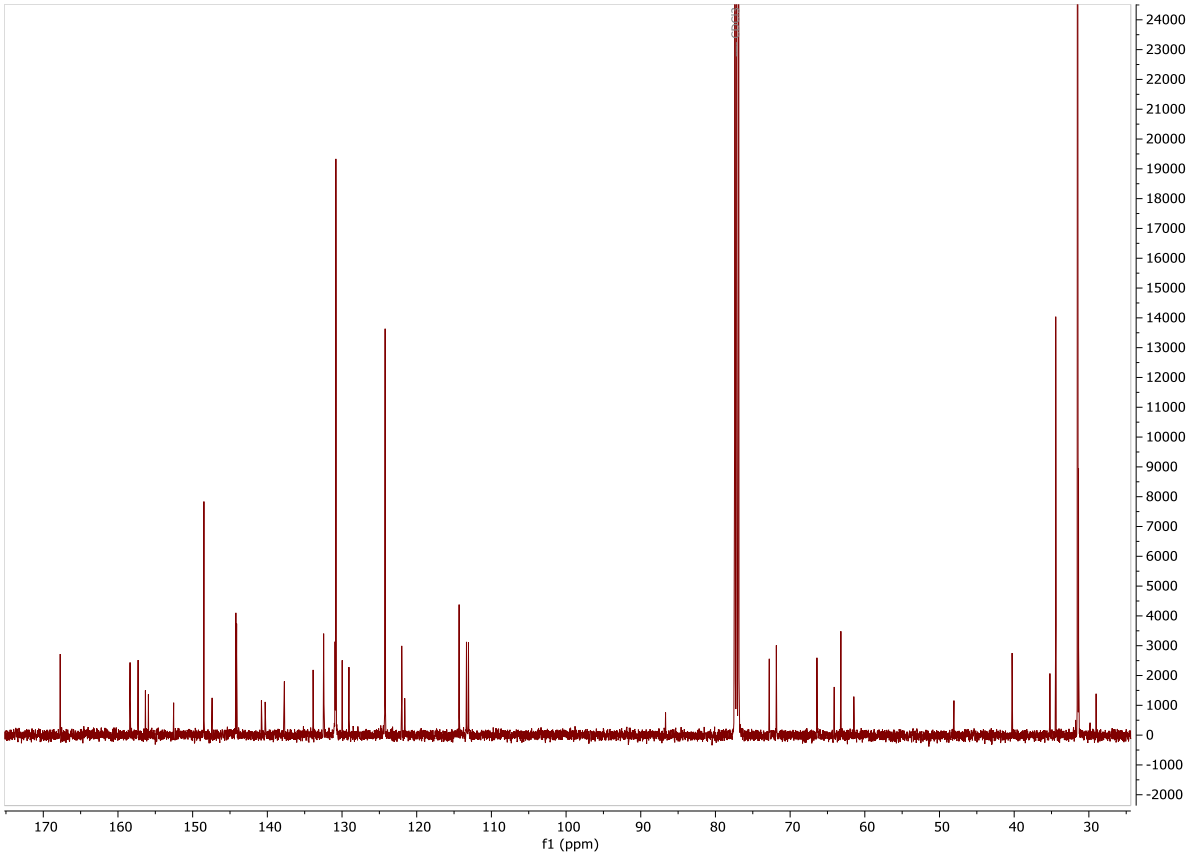

*Figure S1.13: ^{13}C NMR spectrum of Rotaxane **10** (126 MHz, 298 K, $CDCl_3$).*

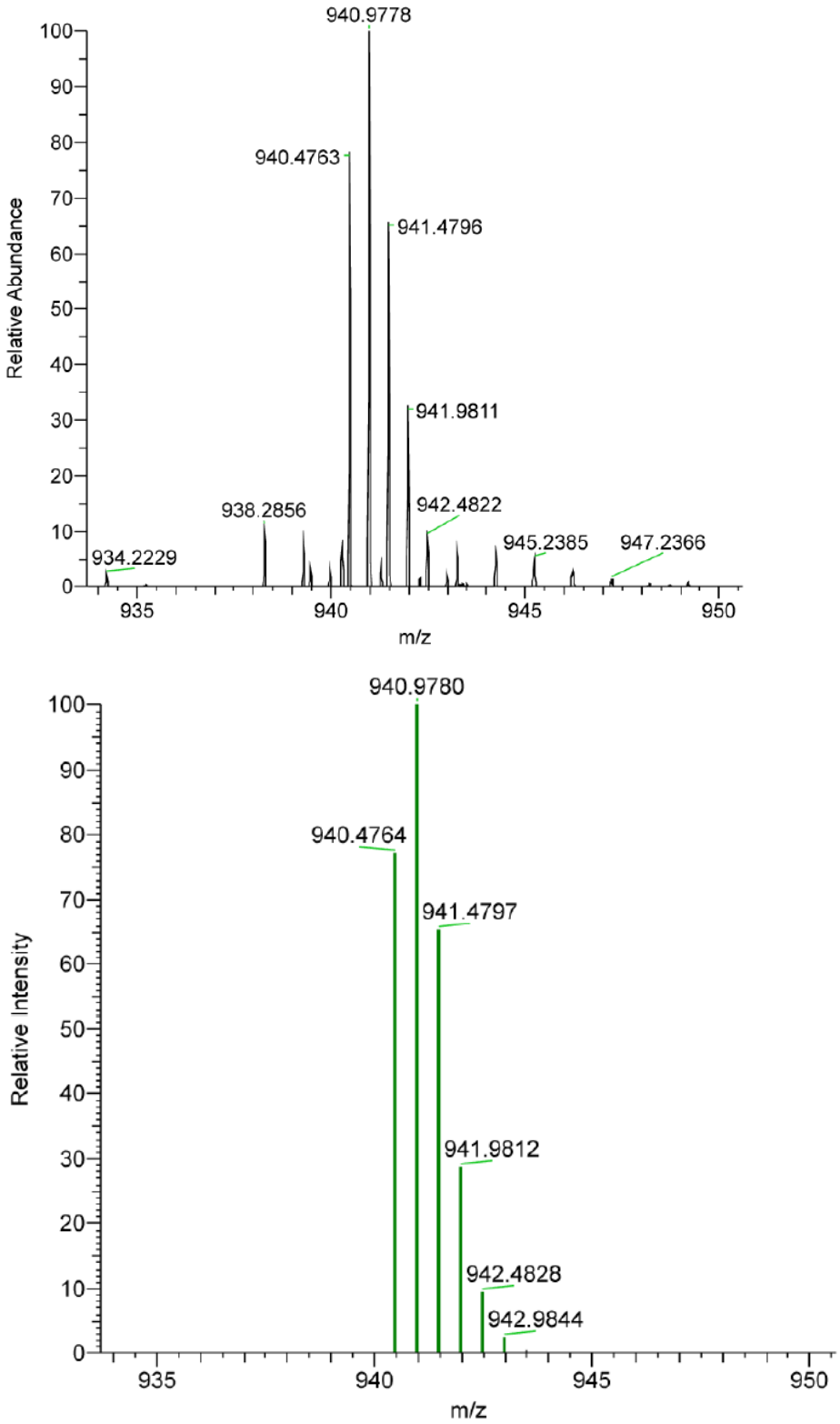

*Figure S1.14: High resolution ESI mass spectrum of Rotaxane **10** (top) and its theoretical spectrum (bottom)*

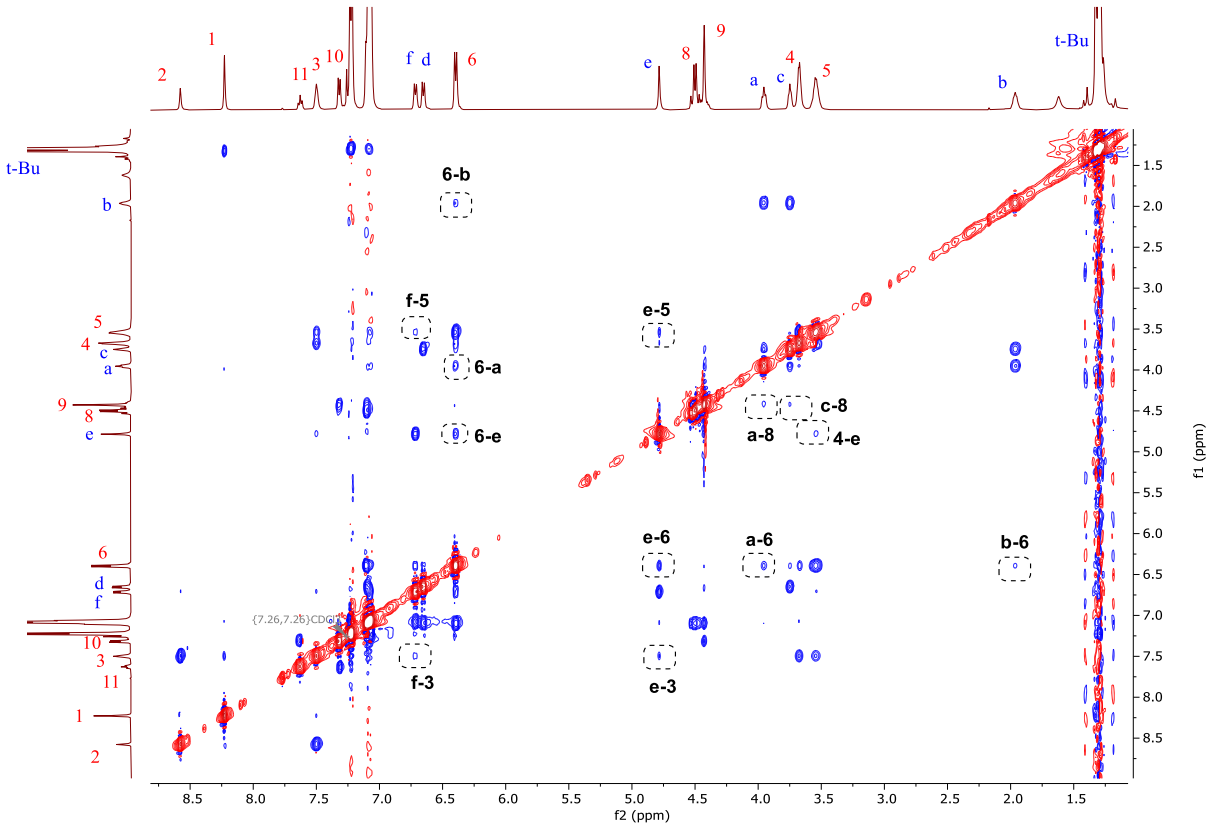

*Figure S1.15: ^{1}H-^{1}H ROESY NMR spectrum of the Rotaxane **10** ($CDCl_3$, 500 MHz, 298 K). Selected cross-peaks arising from through-space interactions of the interlocked macrocycle and axle components of the rotaxane are circled.*

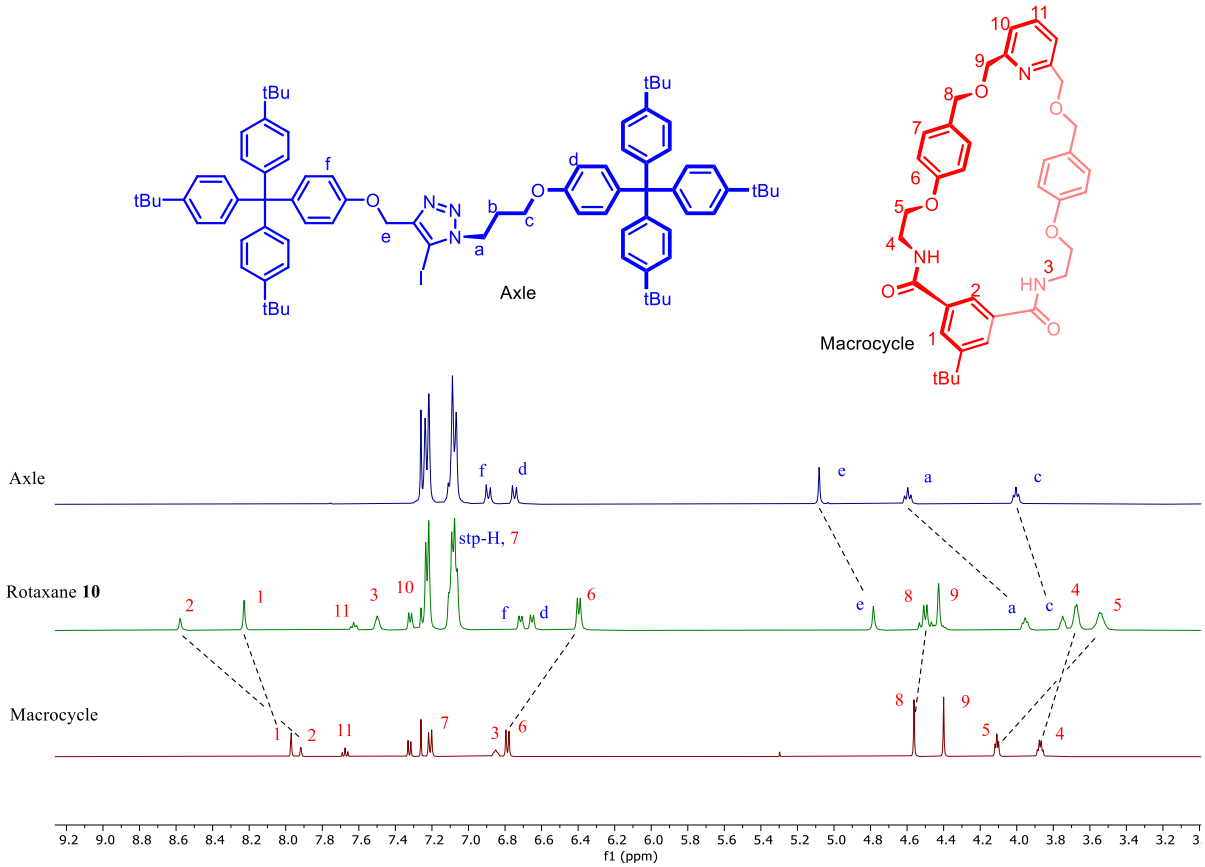

*Figure 1.16: Comparison of ^{1}H NMR spectra of axle (top), rotaxane **10** (middle) and macrocycle (bottom) ($CDCl_3$, 500 MHz, 298 K)*

S2. Solid State Structures

Single crystals of ion-pair bound rotaxane **10·HCl** suitable for X-ray analysis was each coated with Paratone-N oil, suspended in a small fiber loop, and placed in a cold gaseous nitrogen stream on an Oxford Diffraction Supernova X-ray diffractometer performing ϕ- and ω-scans at 150(2) K. Diffraction intensities were measured using graphite monochromated Cu $K\alpha$ radiation (λ = 1.54184 Å). Data collection, indexing, initial cell refinements, frame integration, final cell refinements and absorption corrections were accomplished using the program CrysAlisPro. Scattering factors and anomalous dispersion corrections were taken from the *International Tables for X-ray Crystallography*. The structure was solved by direct methods using SHELXS[6] and refined against F^2 on all data by full-matrix least squares with SHELXL[7] following established refinement strategies.

All non-hydrogen atoms were refined anisotropically. All hydrogen atoms binding to carbon were included into the model at geometrically calculated positions and refined using a riding model. The isotropic displacement parameters of all hydrogen atoms were fixed to 1.2 times the U value of the atoms they are linked to (1.5 times for methyl groups). Details of the data quality and a summary of the residual values for the refinements are listed in Table 2.1.

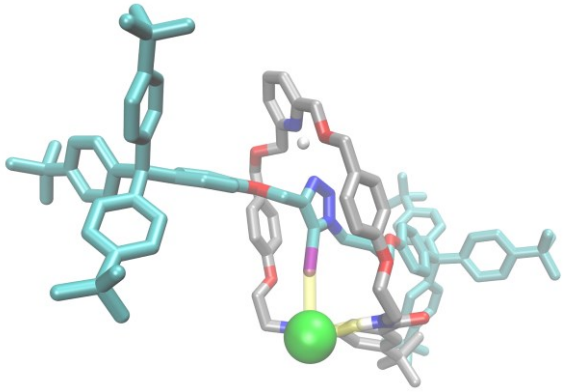

*Figure S2.1: Crystal structure of axle separated HCl-bound R.**10**. Colour code of atoms: O-red, N-blue, I-purple, Cl-green, H-white, C(axle) – teal, C(MC)-gray. Non-covalent host-guest interactions are shown in yellow.*

*Table 2.1: Crystal data and structure refinement for heteroditopic rotaxane **10**·HCl*

Identification code	Rotaxane **10**.HCl	
Empirical formula	C117 H136 Cl I N6 O8	
Formula weight	1916.66	
Temperature	150(2) K	
Wavelength	1.54184 Å	
Crystal system	Triclinic	
Space group	P-1	
Unit cell dimensions	a = 15.1239(2) Å	α = 80.7200(10)°
	b = 15.2550(3) Å	β = 79.3540(10)°
	c = 29.0440(4) Å	γ = 72.2440(10)°
Volume	6232.31(18) $Å^3$	
Z	2	
Density (calculated)	1.021 Mg/m^3	
Absorption coefficient	2.600 mm^{-1}	
F(000)	2028	
Crystal size	0.4 x 0.2 x 0.15 mm^3	
Theta range for data collection	3.588 to 76.634°.	
Index ranges	-19<=h<=18, -19<=k<=16, -36<=l<=35	
Reflections collected	135494	
Independent reflections	25857 [R(int) = 0.0708]	
Completeness to theta = 67.684°	100.0 %	
Absorption correction	Semi-empirical from equivalents	
Max. and min. transmission	1.00000 and 0.18761	
Refinement method	Full-matrix least-squares on F^2	
Data / restraints / parameters	25857 / 0 / 1219	
Goodness-of-fit on F^2	1.045	
Final R indices [I>2sigma(I)]	R1 = 0.0492, wR2 = 0.1375	
R indices (all data)	R1 = 0.0557, wR2 = 0.1441	
Largest diff. peak and hole	1.852 and -1.268 e.$Å^{-3}$	

S3. ^{1}H NMR binding studies

S3.1. General Procedure

All ^{1}H NMR titrations were performed on a Bruker Avance III 500 MHz NMR spectrometer, at 298 K, in $CDCl_3$:CD_3CN solvent mixtures. Initial sample volume of the NMR tube was 0.5 mL whilst concentrations were 1.0 mM of the receptor. Anions were added as their TBA salts and lithium was added as its ClO_4^- salt.

In a typical titration with cation bound receptor, uncomplexed receptor was dissolved in the respective CD_3CN:$CDCl_3$ solvent mixtures containing an equimolar of $LiClO_4$. Resultant mixture was sonicated. TBA salt of the anion was dissolved in the same CD_3CN:$CDCl_3$ solvent ratio to make a 0.05 M TBAX solution. TBAX was added in aliquots to the lithium bound receptor solution and 17 spectra were recorded upon addition of 0.0, 0.2, 0.4, 0.6, 0.8, 1.0, 1.2, 1.4, 1.6, 1.8, 2.0, 2.5, 3.0, 4.0, 5.0, 7.0, 10.0 equivalents of TBAX salt. In all instances, binding of the anion and cation was in fast exchange, allowing the calculation association constants using Bindfit program available from http://supramolecular.org.[8]

^{1}H NMR titrations of rotaxane **9**

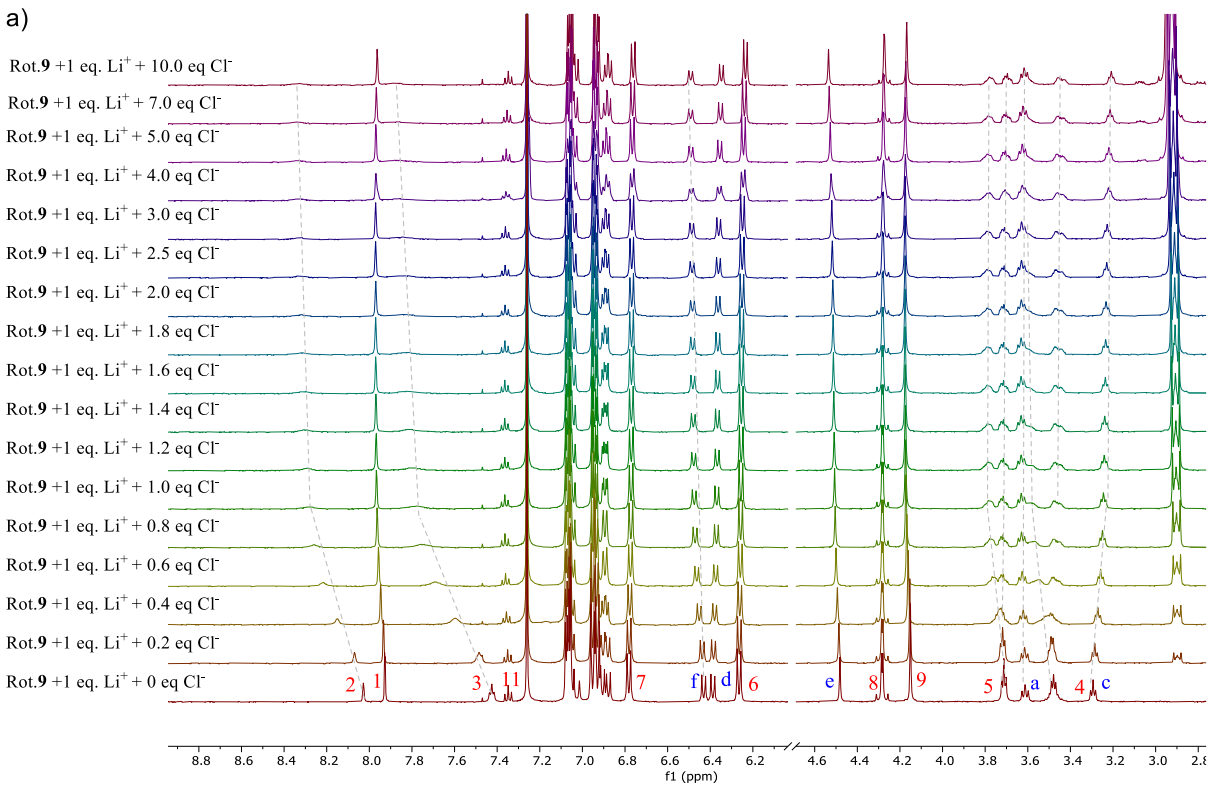

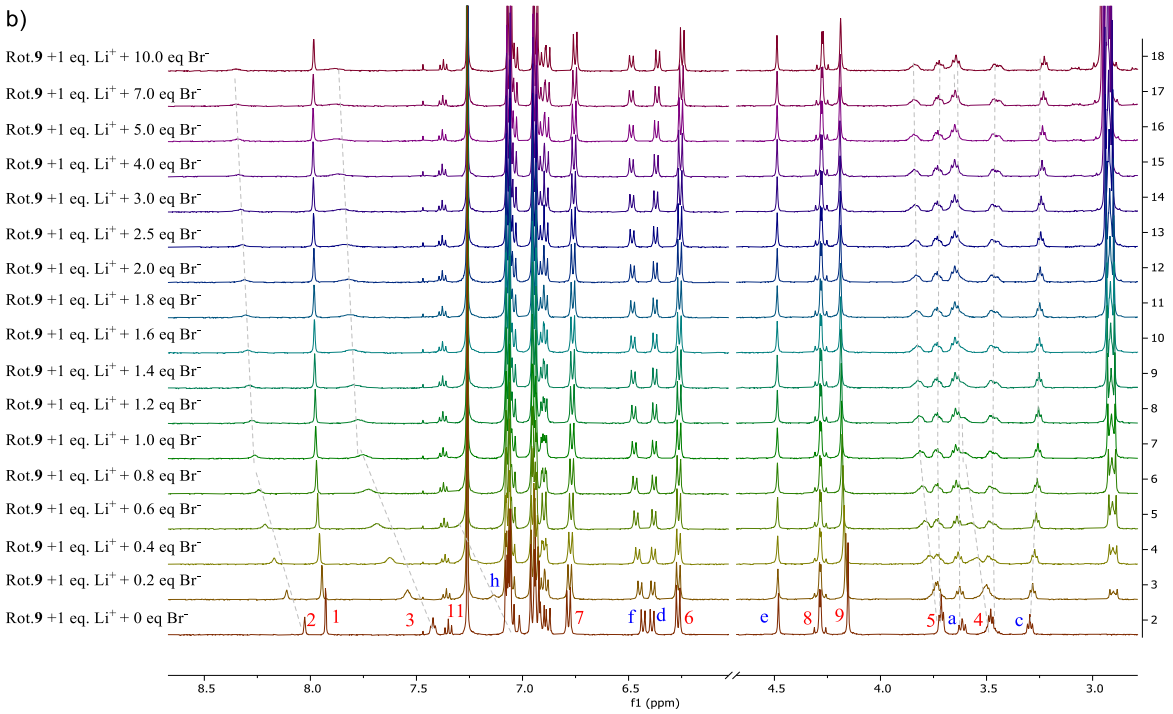

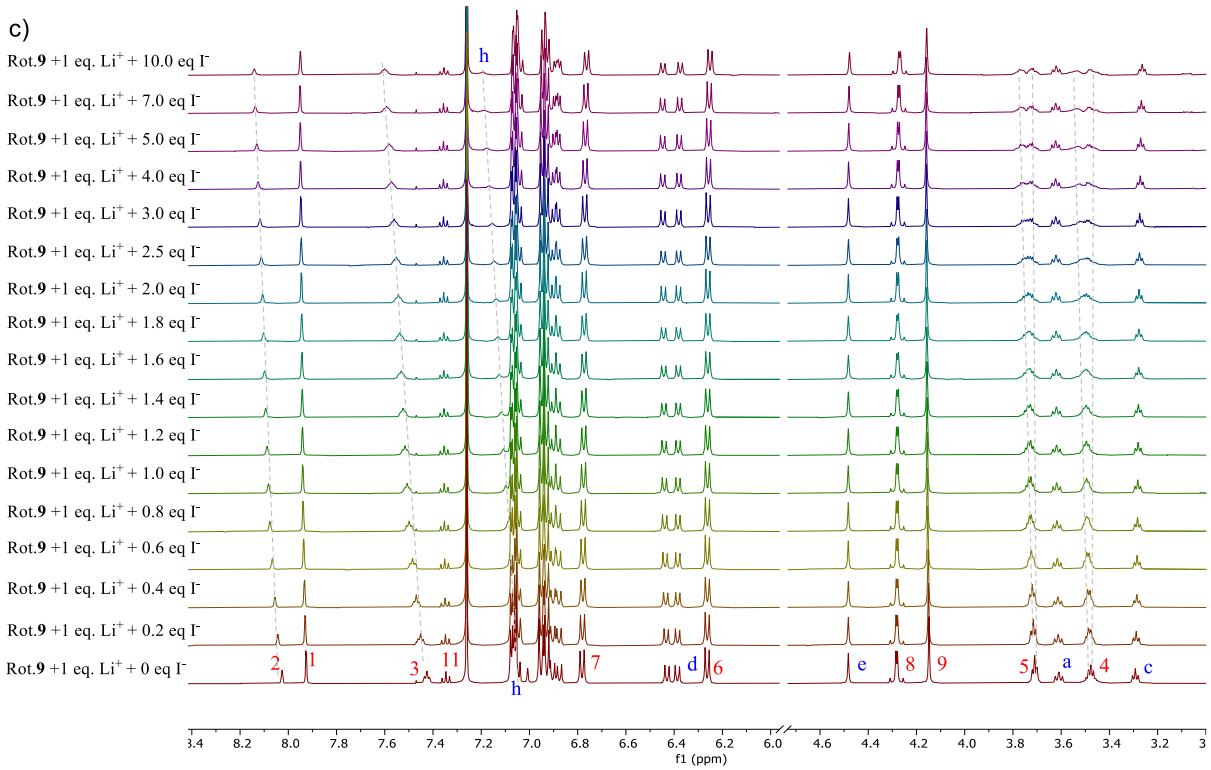

*Figure S3.1: Truncated ^{1}H NMR titration spectra of lithium precomplexed rotaxane **9** upon addition of (a)TBACl,* (b) TBABr and (c) TBAI (500 MHz, 298 K, 7:3 $CDCl_3$:CD_3CN, [Rot.**9**] = 1.0 mM).*H_h proton peak shifts are not visible presumably due to strong HB interactions with Cl^-, resulting in peak broadening. (Connecting lines are to guide the eye only)*

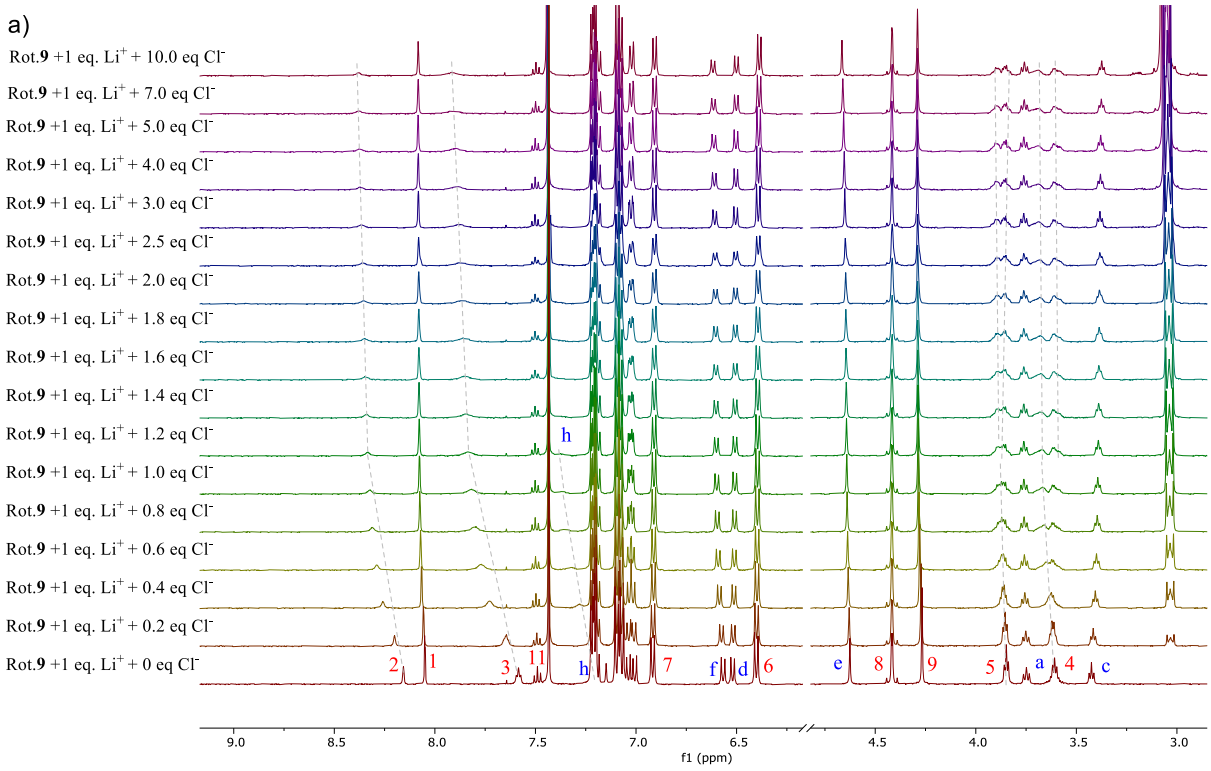

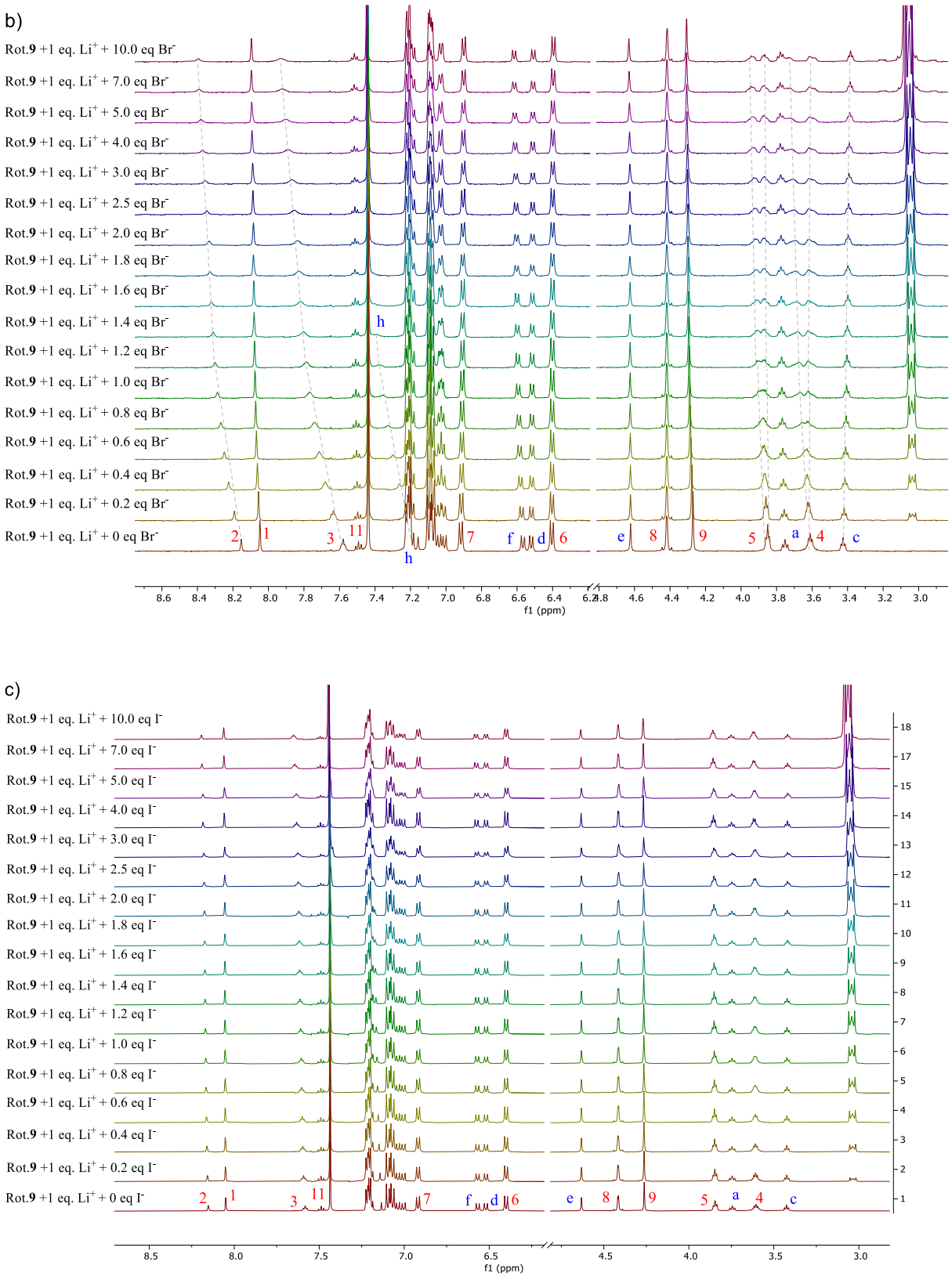

*Figure S3.2: Truncated ^{1}H NMR titration spectra of lithium precomplexed rotaxane **9** upon addition of (a)TBACl, (b) TBABr and (c) TBAI (500 MHz, 298 K, 6:4 $CDCl_3$:CD_3CN, [Rot.**9**] = 1.0 mM). (Connecting lines are to guide the eye only)*

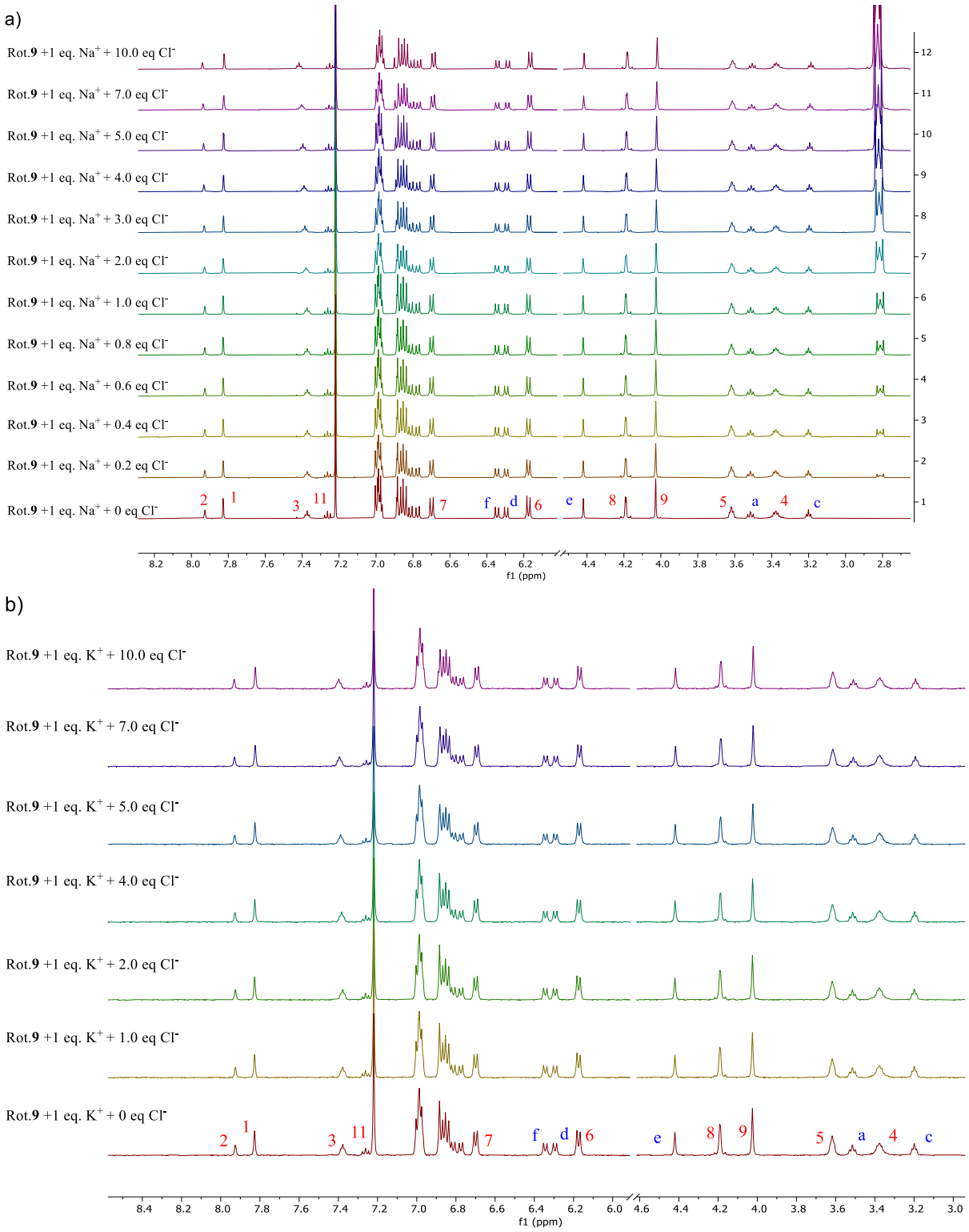

*Figure S3.3: Truncated ^{1}H NMR titration spectra of a) sodium precomplexed rotaxane **9** upon addition of TBACl, (b) Potassium precomplexed rotaxane **9** upon addition of TBACl (500 MHz, 298 K, 6:4 $CDCl_3$:CD_3CN, [Rot.**9**] = 1.0 mM). K^+ and Na^+ were added as their ClO_4^- salts as it was soluble in the required concentration of 1mM. (Connecting lines are to guide the eye only).*

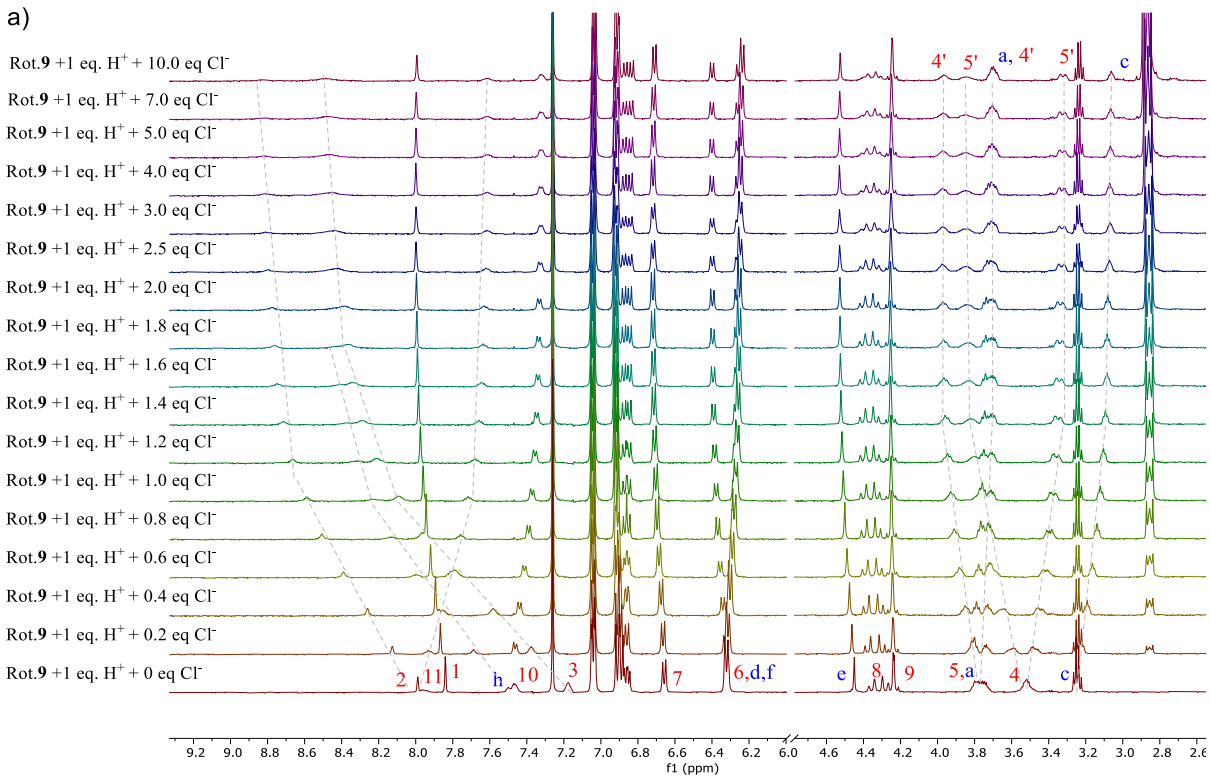
a)
Rot.9 +1 eq. H+ + 10.0 eq Cl-
Rot.9 +1 eq. H+ + 7.0 eq Cl-
Rot.9 +1 eq. H+ + 5.0 eq Cl-
Rot.9 +1 eq. H+ + 4.0 eq Cl-
Rot.9 +1 eq. H+ + 3.0 eq Cl-
Rot.9 +1 eq. H+ + 2.5 eq Cl-
Rot.9 +1 eq. H+ + 2.0 eq Cl-
Rot.9 +1 eq. H+ + 1.8 eq Cl-
Rot.9 +1 eq. H+ + 1.6 eq Cl-
Rot.9 +1 eq. H+ + 1.4 eq Cl-
Rot.9 +1 eq. H+ + 1.2 eq Cl-
Rot.9 +1 eq. H+ + 1.0 eq Cl-
Rot.9 +1 eq. H+ + 0.8 eq Cl-
Rot.9 +1 eq. H+ + 0.6 eq Cl-
Rot.9 +1 eq. H+ + 0.4 eq Cl-
Rot.9 +1 eq. H+ + 0.2 eq Cl-
Rot.9 +1 eq. H+ + 0 eq Cl-
4' 5' a, 4' 5' c
2 11 1 h 10 3 7 6,d,f
e 8 9 5,a 4 c
9.2 9.0 8.8 8.6 8.4 8.2 8.0 7.8 7.6 7.4 7.2 7.0 6.8 6.6 6.4 6.2 6.0 4.6 4.4 4.2 4.0 3.8 3.6 3.4 3.2 3.0 2.8
f1 (ppm)

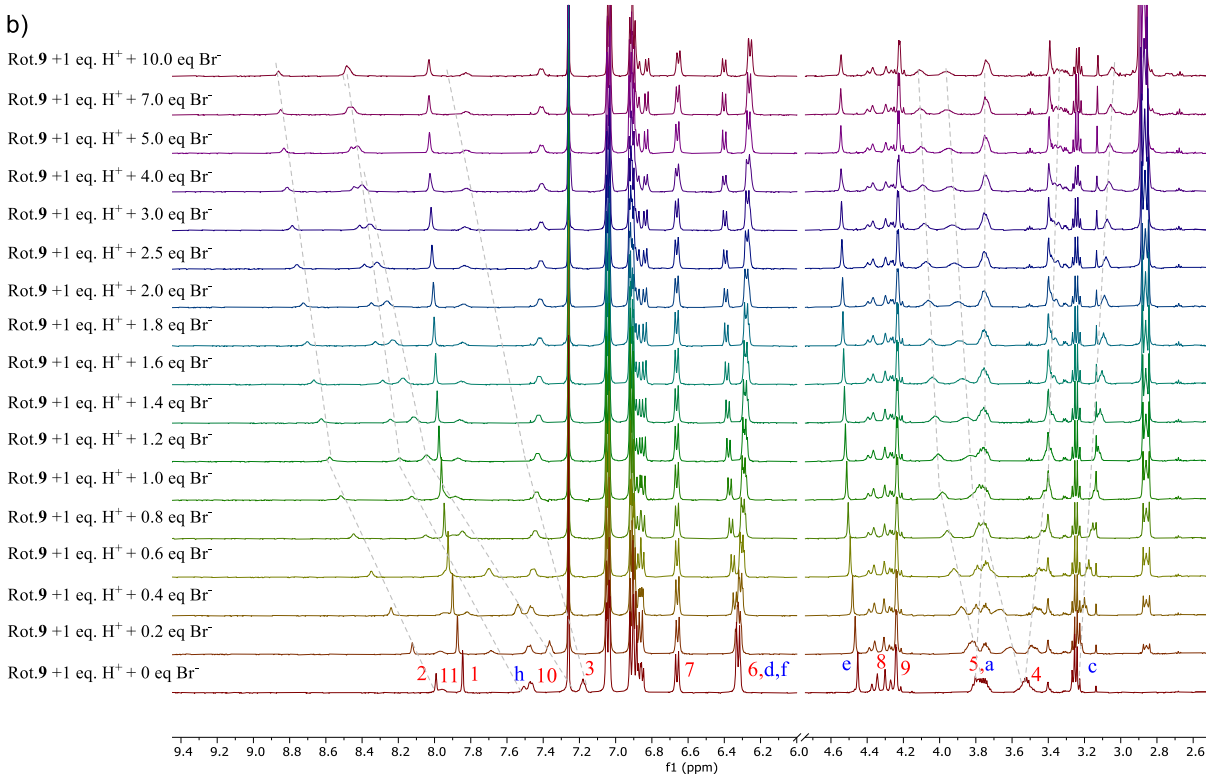
b)
Rot.9 +1 eq. H+ + 10.0 eq Br-
Rot.9 +1 eq. H+ + 7.0 eq Br-
Rot.9 +1 eq. H+ + 5.0 eq Br-
Rot.9 +1 eq. H+ + 4.0 eq Br-
Rot.9 +1 eq. H+ + 3.0 eq Br-
Rot.9 +1 eq. H+ + 2.5 eq Br-
Rot.9 +1 eq. H+ + 2.0 eq Br-
Rot.9 +1 eq. H+ + 1.8 eq Br-
Rot.9 +1 eq. H+ + 1.6 eq Br-
Rot.9 +1 eq. H+ + 1.4 eq Br-
Rot.9 +1 eq. H+ + 1.2 eq Br-
Rot.9 +1 eq. H+ + 1.0 eq Br-
Rot.9 +1 eq. H+ + 0.8 eq Br-
Rot.9 +1 eq. H+ + 0.6 eq Br-
Rot.9 +1 eq. H+ + 0.4 eq Br-
Rot.9 +1 eq. H+ + 0.2 eq Br-
Rot.9 +1 eq. H+ + 0 eq Br-
2 11 1 h 10 3 7 6,d,f
e 8 9 5,a 4 c
9.4 9.2 9.0 8.8 8.6 8.4 8.2 8.0 7.8 7.6 7.4 7.2 7.0 6.8 6.6 6.4 6.2 6.0 4.6 4.4 4.2 4.0 3.8 3.6 3.4 3.2 3.0 2.8 2.6
f1 (ppm)

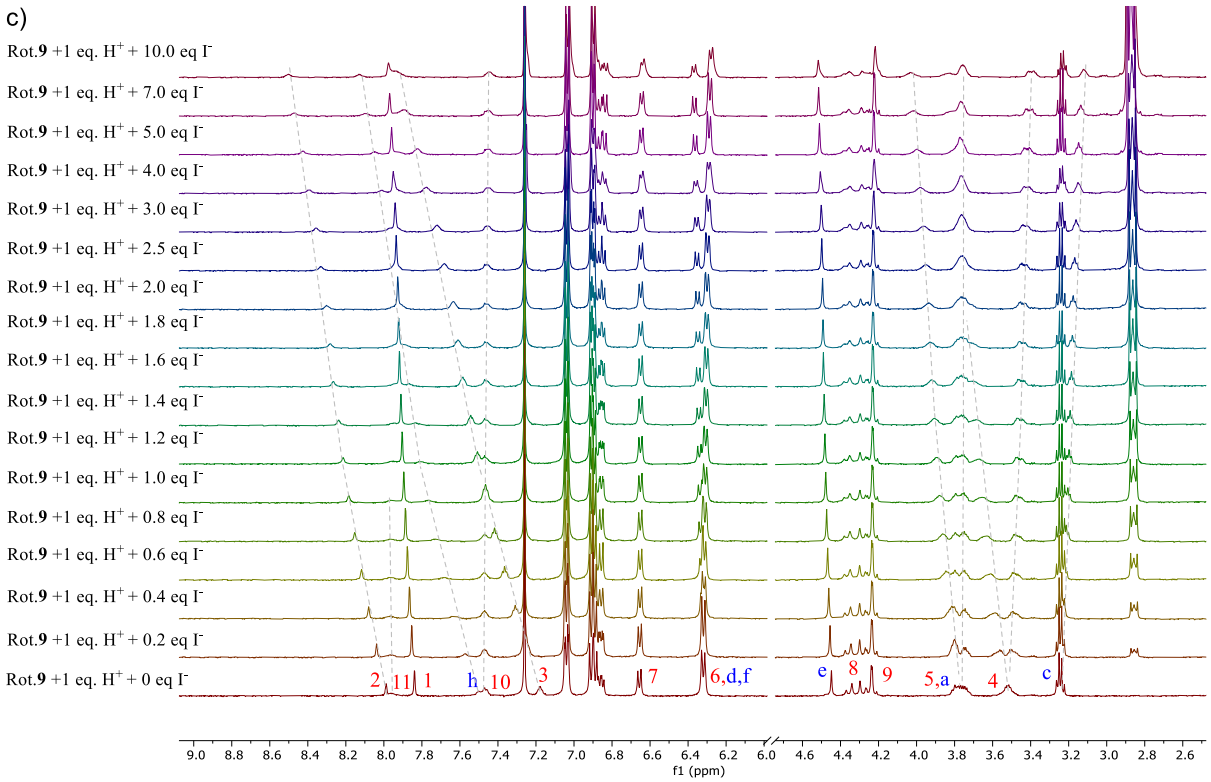

*Figure S3.4: Truncated ^{1}H NMR titration spectra of H^{+} precomplexed rotaxane **9** upon addition of (a)TBACl, (b) TBABr and (c) TBAI (500 MHz, 298 K, 6:4 $CDCl_3$:CD_3CN, [Rot.**10**] = 1.0 mM). (Connecting lines are to guide the eye only)*

^{1}H NMR titrations of Rotaxane **10**

a)

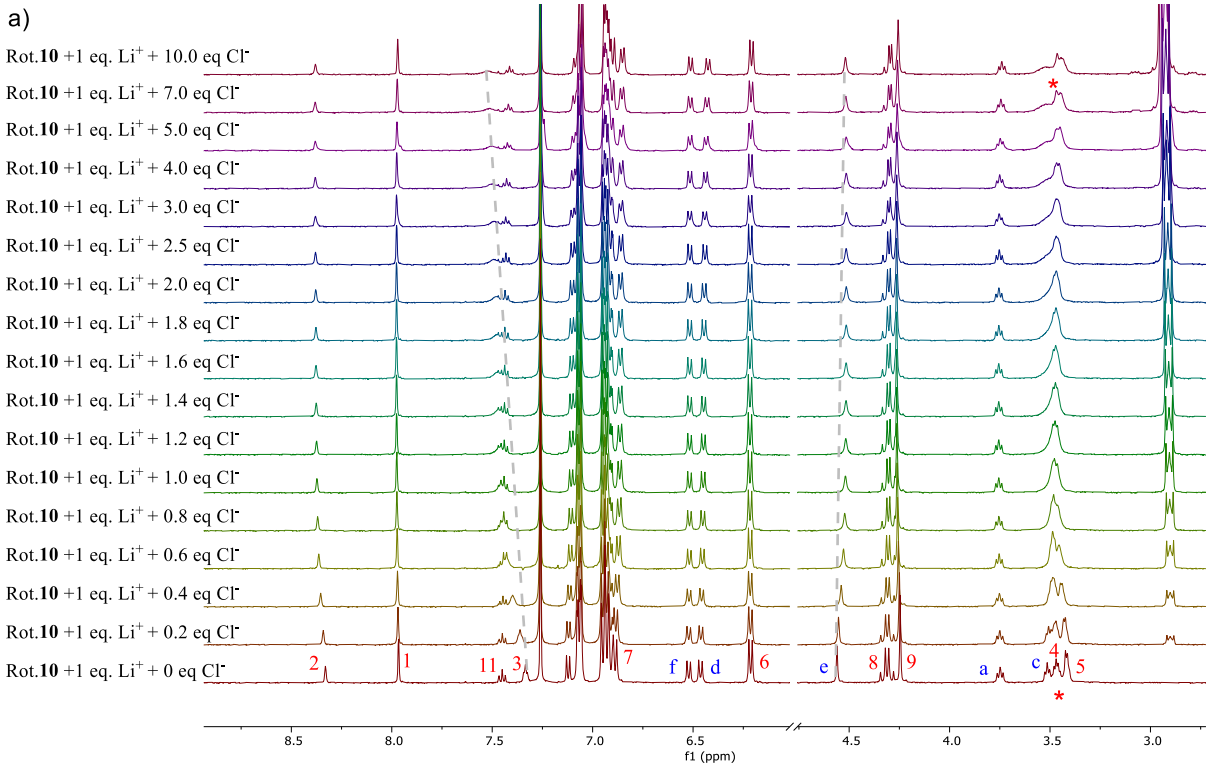

b)

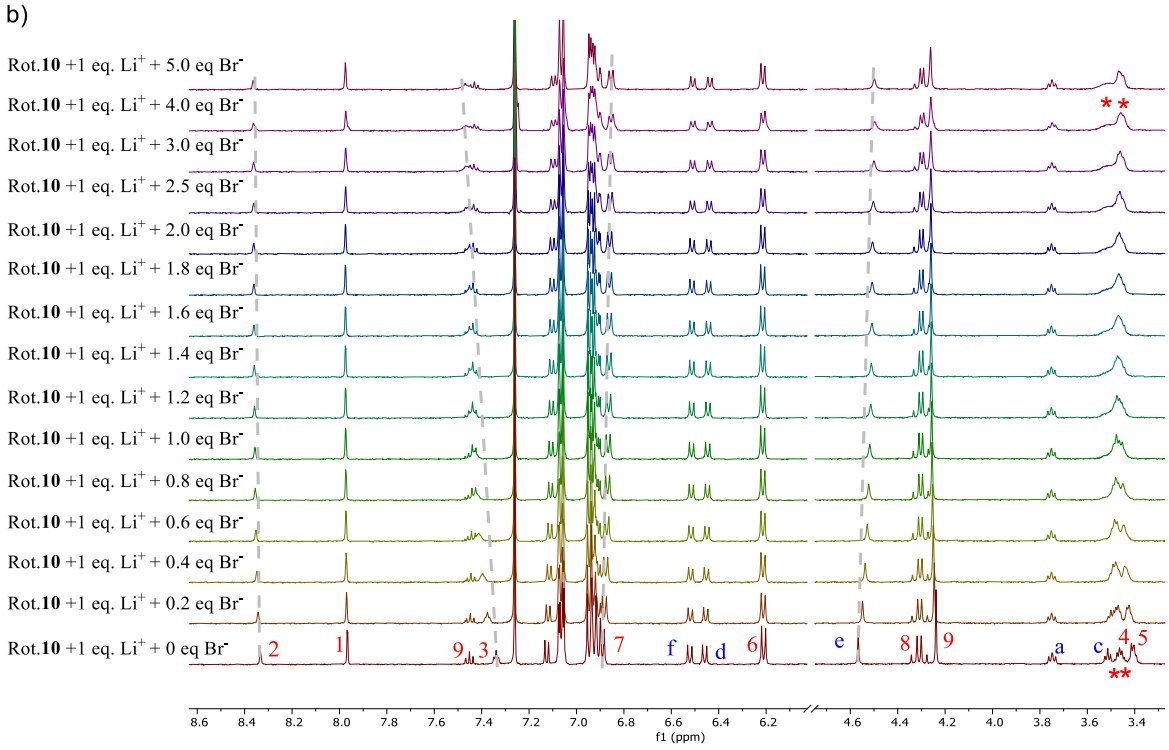

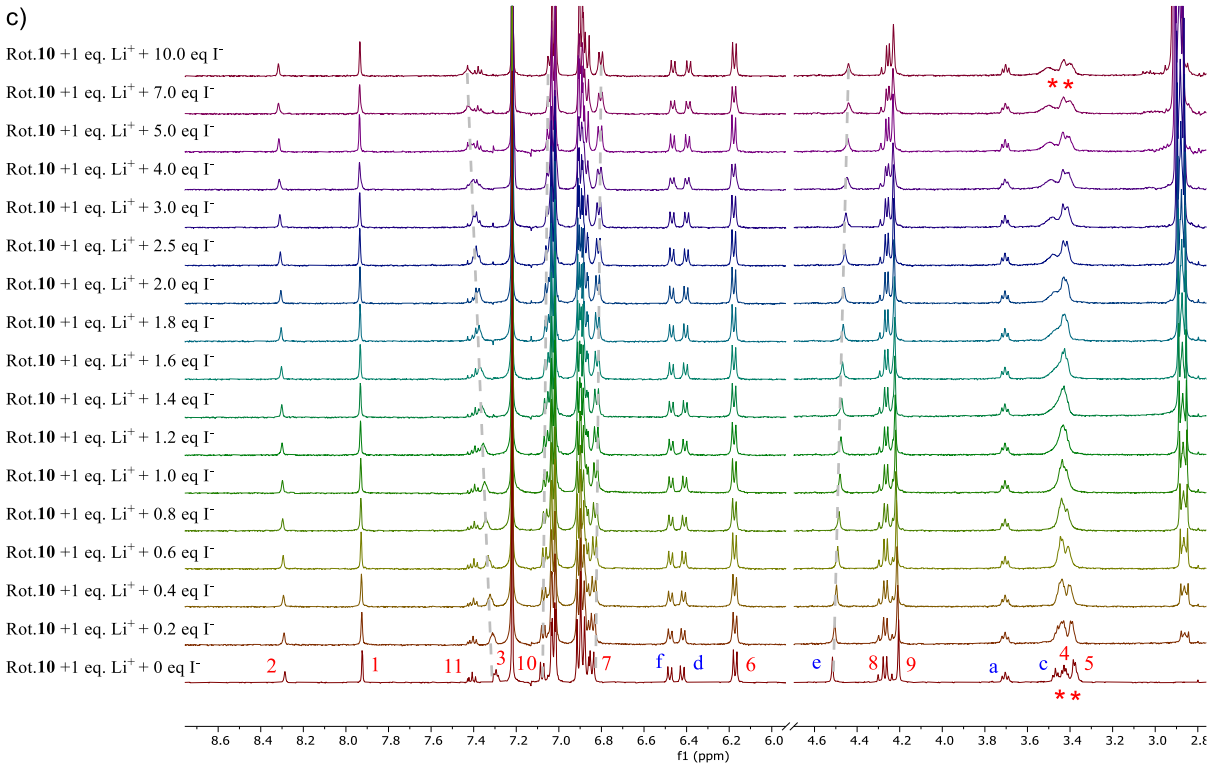

*Figure S3.5: Truncated ^{1}H NMR titration spectra of lithium precomplexed rotaxane **10** upon addition of (a)TBACl, (b) TBABr* and (c) TBAI (500 MHz, 298 K, 7:3 $CDCl_3$:CD_3CN, [Rot.**10**] = 1.0 mM). *due to demetallation, the determination of apparent anion association constants only used data points up to and including the addition of 5 eq. of TBABr (Connecting lines are to guide the eye only)*

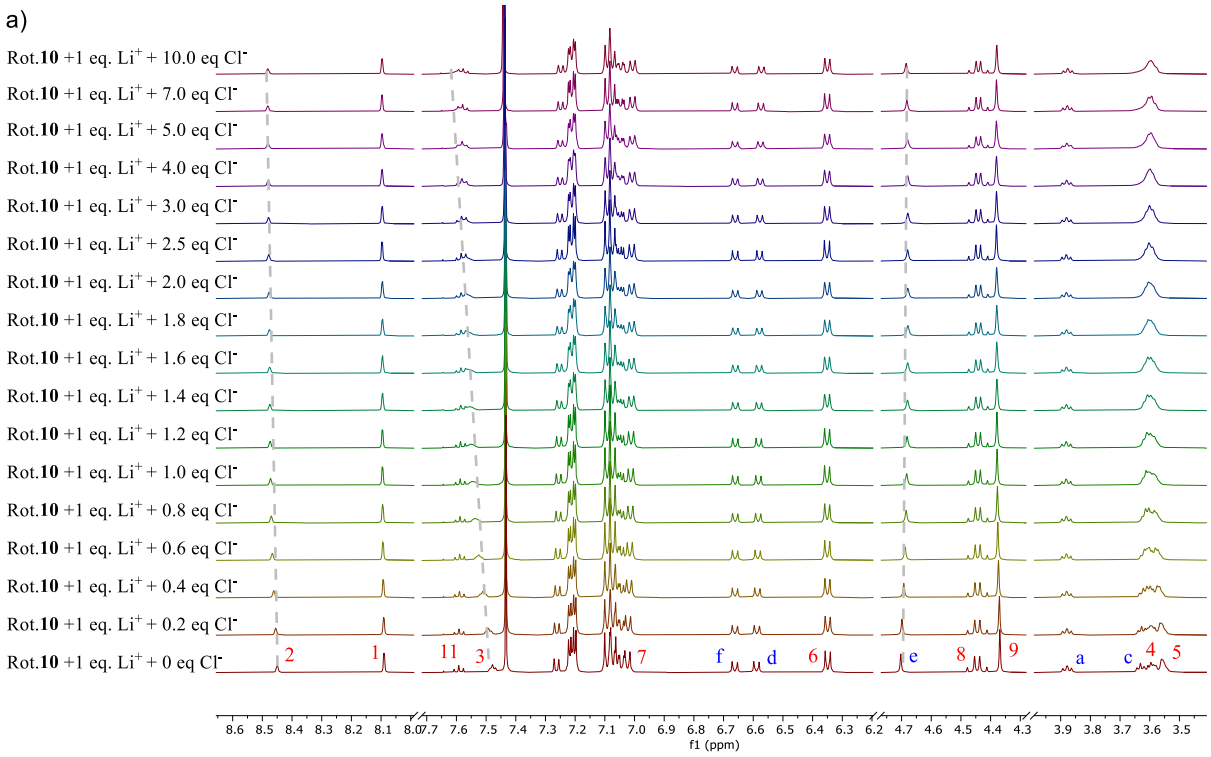

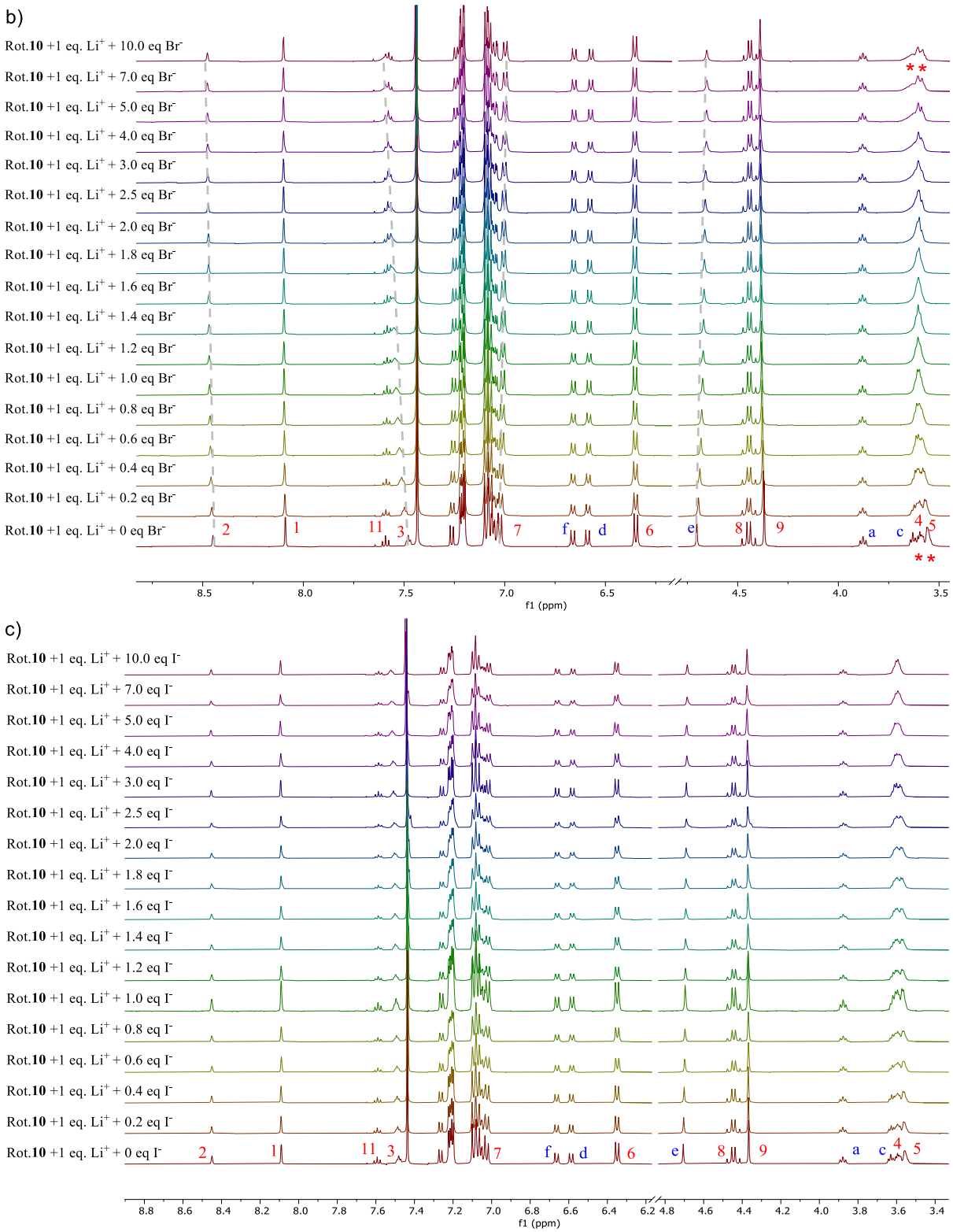

*Figure S3.6: Truncated ^{1}H NMR titration spectra of lithium precomplexed rotaxane **10** upon addition of (a)TBACl, (b) TBABr and (c) TBAI (500 MHz, 298 K, 6:4 $CDCl_3$:CD_3CN, [Rot.**10**] = 1.0 mM). (Connecting lines are to guide the eye only)*

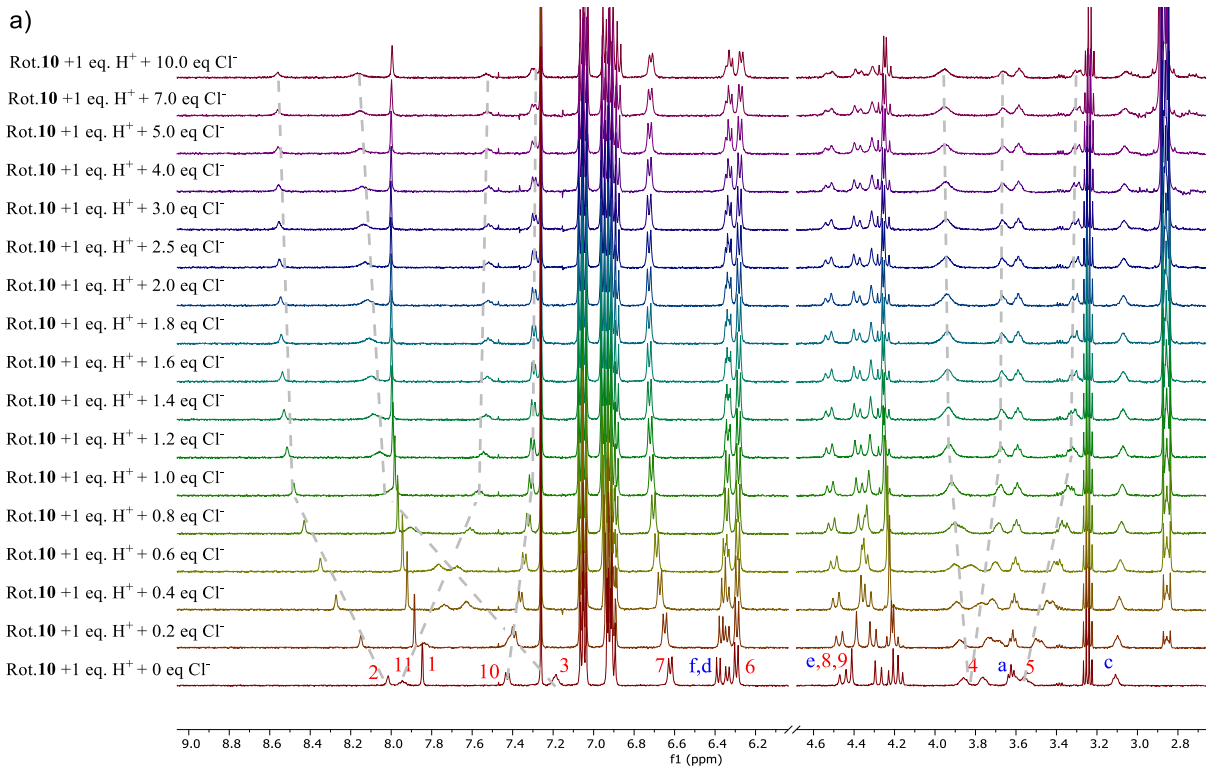
a)
Rot.10 +1 eq. H+ + 10.0 eq Cl-
Rot.10 +1 eq. H+ + 7.0 eq Cl-
Rot.10 +1 eq. H+ + 5.0 eq Cl-
Rot.10 +1 eq. H+ + 4.0 eq Cl-
Rot.10 +1 eq. H+ + 3.0 eq Cl-
Rot.10 +1 eq. H+ + 2.5 eq Cl-
Rot.10 +1 eq. H+ + 2.0 eq Cl-
Rot.10 +1 eq. H+ + 1.8 eq Cl-
Rot.10 +1 eq. H+ + 1.6 eq Cl-
Rot.10 +1 eq. H+ + 1.4 eq Cl-
Rot.10 +1 eq. H+ + 1.2 eq Cl-
Rot.10 +1 eq. H+ + 1.0 eq Cl-
Rot.10 +1 eq. H+ + 0.8 eq Cl-
Rot.10 +1 eq. H+ + 0.6 eq Cl-
Rot.10 +1 eq. H+ + 0.4 eq Cl-
Rot.10 +1 eq. H+ + 0.2 eq Cl-
Rot.10 +1 eq. H+ + 0 eq Cl-
2
11
1
10
3
7
f,d
6
e,8,9
4
a
5
c
9.0 8.8 8.6 8.4 8.2 8.0 7.8 7.6 7.4 7.2 7.0 6.8 6.6 6.4 6.2
4.6 4.4 4.2 4.0 3.8 3.6 3.4 3.2 3.0 2.8
f1 (ppm)

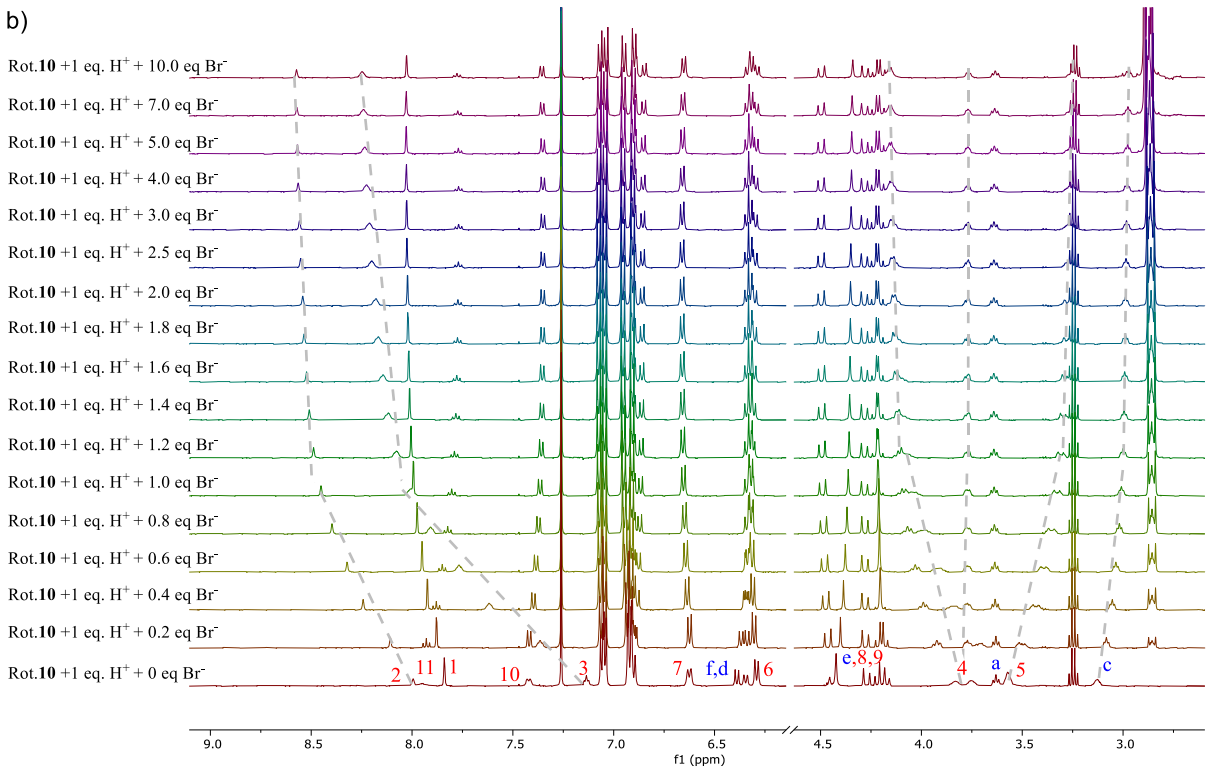
b)
Rot.10 +1 eq. H+ + 10.0 eq Br-
Rot.10 +1 eq. H+ + 7.0 eq Br-
Rot.10 +1 eq. H+ + 5.0 eq Br-
Rot.10 +1 eq. H+ + 4.0 eq Br-
Rot.10 +1 eq. H+ + 3.0 eq Br-
Rot.10 +1 eq. H+ + 2.5 eq Br-
Rot.10 +1 eq. H+ + 2.0 eq Br-
Rot.10 +1 eq. H+ + 1.8 eq Br-
Rot.10 +1 eq. H+ + 1.6 eq Br-
Rot.10 +1 eq. H+ + 1.4 eq Br-
Rot.10 +1 eq. H+ + 1.2 eq Br-
Rot.10 +1 eq. H+ + 1.0 eq Br-
Rot.10 +1 eq. H+ + 0.8 eq Br-
Rot.10 +1 eq. H+ + 0.6 eq Br-
Rot.10 +1 eq. H+ + 0.4 eq Br-
Rot.10 +1 eq. H+ + 0.2 eq Br-
Rot.10 +1 eq. H+ + 0 eq Br-
2
11
1
10
3
7
f,d
6
e,8,9
4
a
5
c
9.0 8.5 8.0 7.5 7.0 6.5
4.5 4.0 3.5 3.0
f1 (ppm)

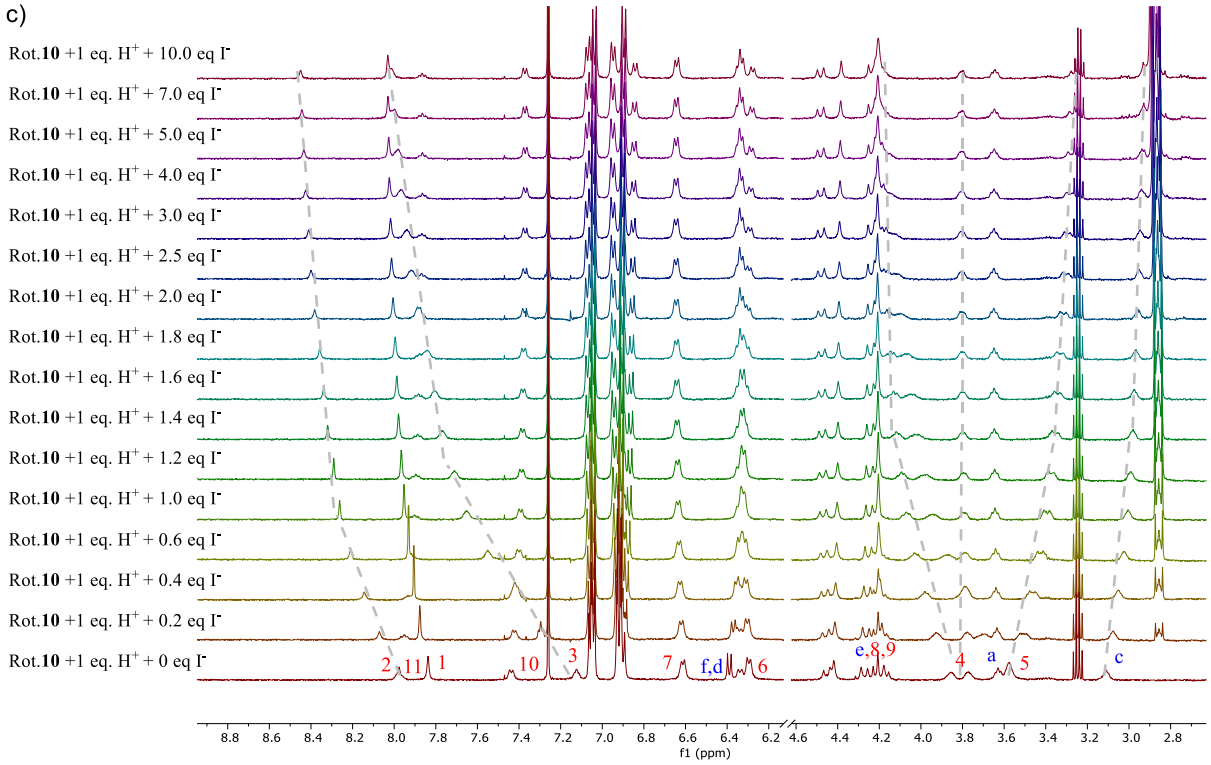

*Figure S3.7: Truncated ^{1}H NMR titration spectra of H^{+} precomplexed rotaxane **10** upon addition of (a)TBACl, (b) TBABr and (c) TBAI (500 MHz, 298 K, 6:4 $CDCl_3$:CD_3CN, [Rot.**10**] = 1.0 mM). (Connecting lines are to guide the eye only)*

^{1}H NMR titrations of macrocycle **6**

Addition of $LiClO_4$ to the macrocycle resulted perturbations in protons H_9 and H_{10}, suggesting Li^+ coordination to the pyridyl motif. Subsequent addition of TBA halide salts caused significant downfield shifts in the internal benzene proton H_2 and amide protons H_3 indicating anion binding through amide HB donors.

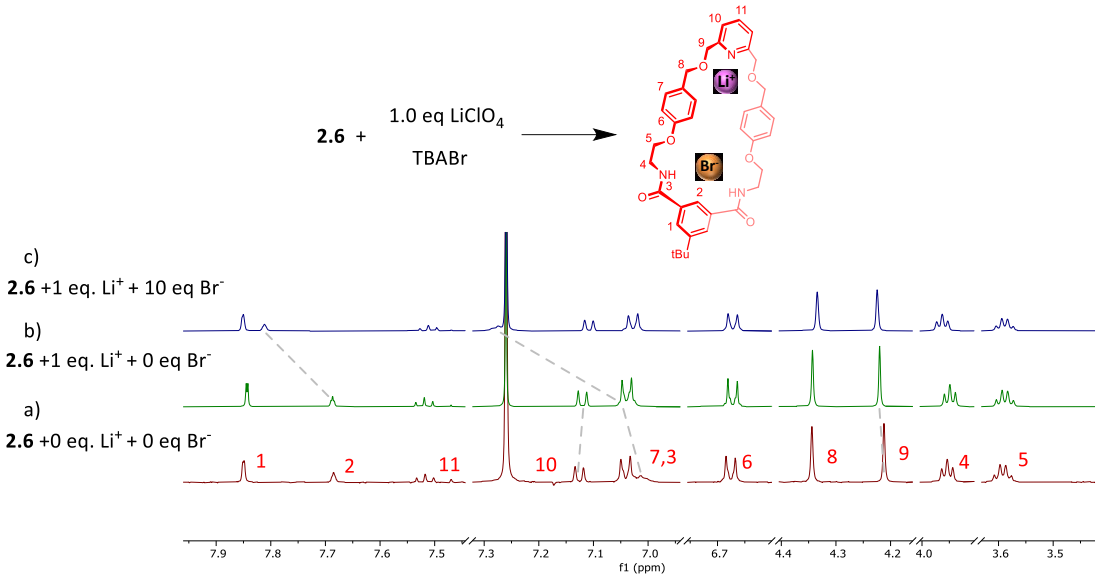

*Figure 3.8: Superimposed ^{1}H NMR spectra in 4:6, CD_3CN-$CDCl_3$, of a) Macrocycle **6**, b) Macrocycle **6** in the presence of 1 eq. of $LiClO_4$, c) Macrocycle **2.6** with further addition of 10 eq. of TBABr.*

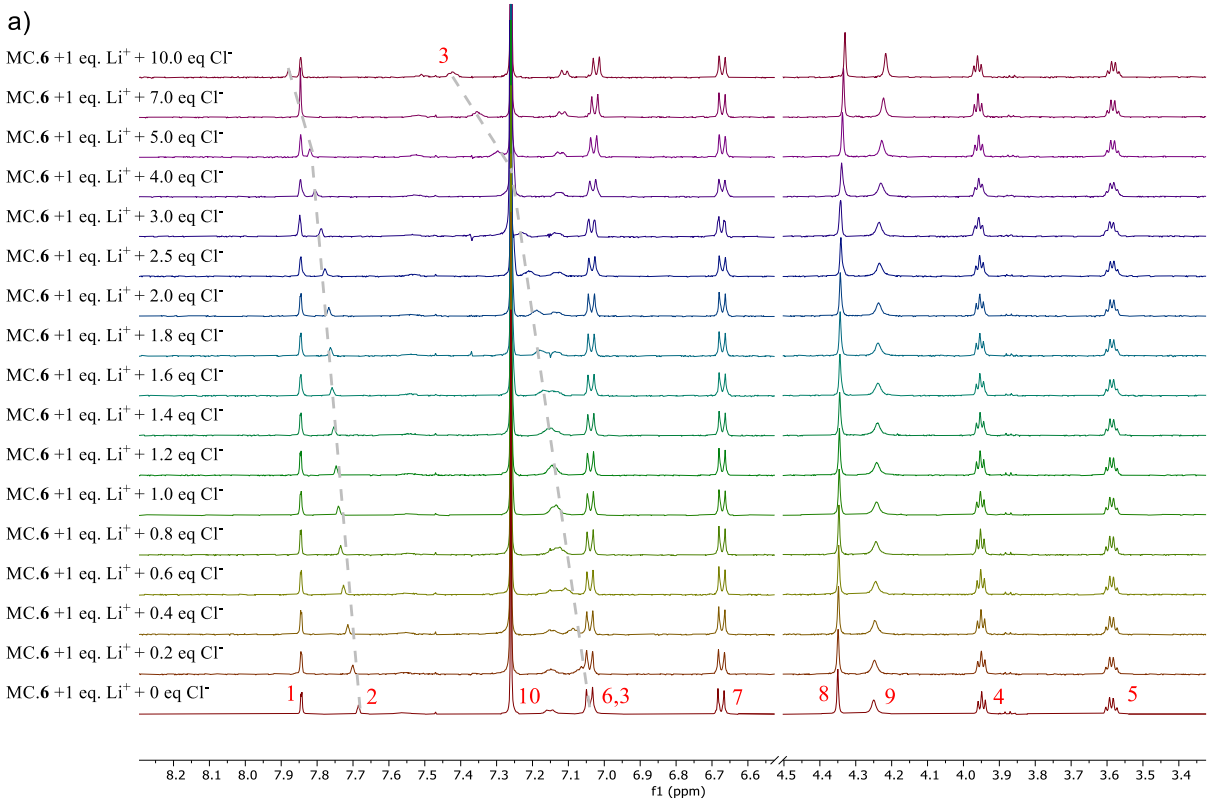

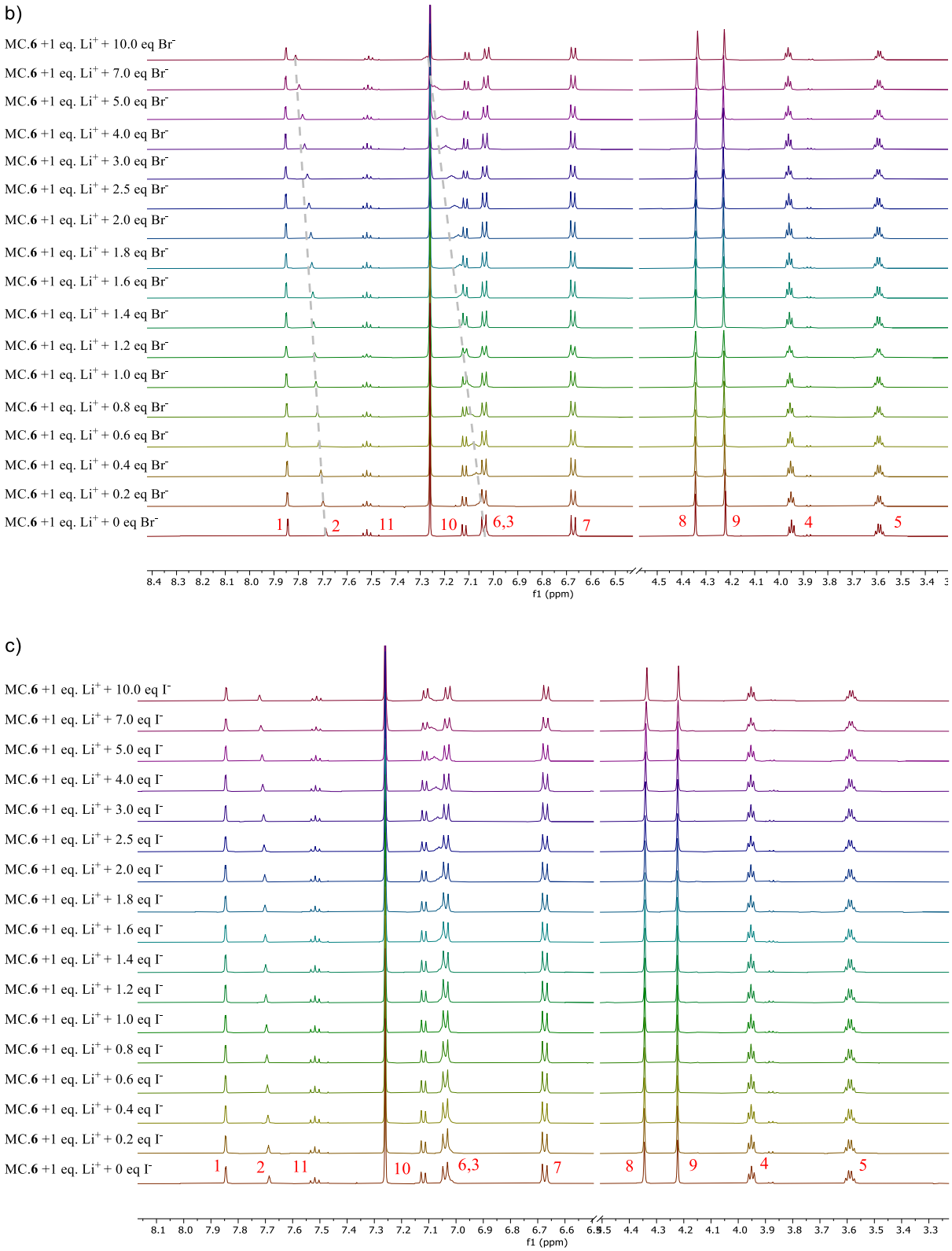

*Figure S3.9: Truncated ^{1}H NMR titration spectra of lithium precomplexed macrocycle **6** upon addition of (a)TBACl, (b) TBABr and (c) TBAI (500 MHz, 298 K, 6:4 $CDCl_3$:CD_3CN, [MC.**6**] = 1.0 mM). (Connecting lines are to guide the eye only)*

S3.2. Cation binding studies with Rotaxane 9

^{1}H NMR cation binding titration experiments were conducted using a similar procedure stated in Section S3.1. Rotaxane **9** was dissolved in a 7:3, $CDCl_3$:CD_3CN solution to make a 0.5 mL of 1 mM solution. $LiClO_4$ was added as the Li^+ source and $NaBAr^F$ as the Na^+ source. A 25 mM solution of $LiClO_4$ was prepared using the same $CDCl_3$:CD_3CN solvent system. The cation solution was sequentially added to the rotaxane solution while recording ^{1}H NMR spectra with each addition. Titration spectra was only recorded till the addition of 4.0 eq of $LiClO_4$ due to precipitation of Rotaxane-Li complex.

In typical lithium ion-pair binding titration experiments, rotaxanes are initially precomplexed with Li^+ by adding 1 equivalent of $LiClO_4$ to the rotaxane. Hence, attention was given to quantify the amount of Li^+ bound to the rotaxane with the addition of 1 equivalent of $LiClO_4$. To this end, a global BindFit analysis was conducted by monitoring non-overlapping peak shifts of H_9, H_e upon sequential addition of the $LiClO_4$, to calculate the association constant of Li^+ with rotaxane **9** to be K_a (Li^+) = 312 (2) M^{-1}.

$K_a(Li^+)$ = 312 M^{-1}
Upon addition of 1.0 equivalent of Li^+ suppose lithium complexed rotaxane moles = x
solvent volume in the NMR tube = v = 0.0005 L
R.**9** moles in NMR tube: 5x10^{-7} mol

$$Rot. + Li^+ \leftrightharpoons Rot\text{-}Li\ complex$$

	Moles (mol)		
	free R.**9**	free Li^+	Li-R.**9** complex
Before adding 1 eq Li^+	5x10^{-7}	-	-
After adding 1 eq Li^+	(5x10^{-7}) - x	(5x10^{-7}) - x	x

$$Ka = \frac{[Li - R.\mathbf{9}]}{[Free\ R.\mathbf{9}][Free\ Li^+]}$$

$$Ka = \frac{x/v}{\left((5 * 10^{-7} - x)/v\right)^2}$$

Solutions of the above quadratic equation, x: x'= 1.0×10^{-7} mol and x''= 2.5×10^{-6} mol
As x''>5×10^{-7} mol, x=x'= 1×10^{-7} mol

$$\text{lithium complexed rotaxane } \% = \left(\frac{1.0*10^{-7}}{5*10^{-7}}\right) 100\% = 20\%$$

Under the conditions of a typical ion-pair titration experiment described in Section S3.1, only approx. 20% of rotaxane is bound to Li^+ while approx. 80% of the rotaxane in solution exists as the uncomplexed neutral rotaxane. However, the apparent anion binding constants were calculated assuming 100% pre-complexation of the Li^+ cation, and therefore are likely an underestimation of the 'true' anion binding affinities of the Li^+-bound rotaxanes.

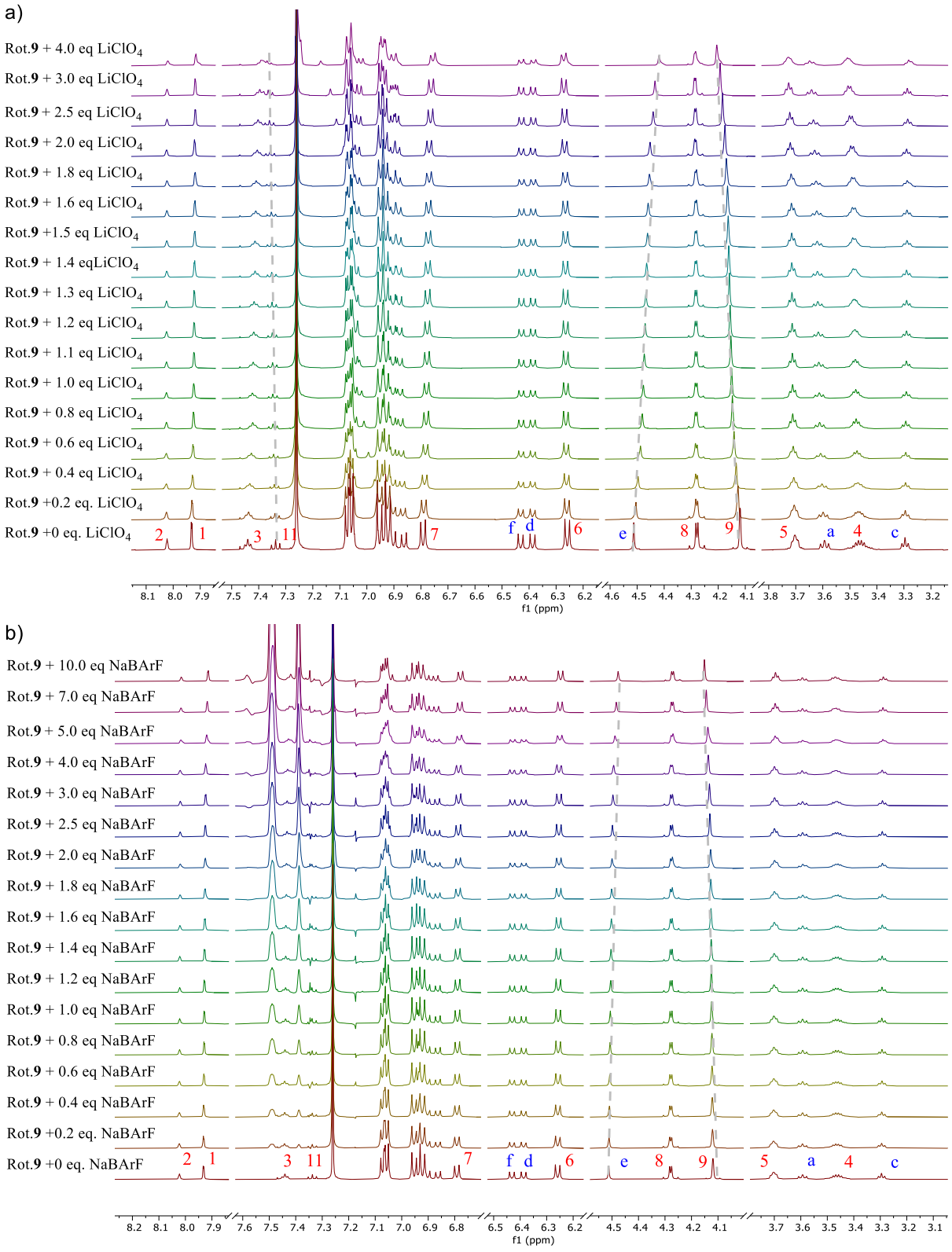

*Figure S3.10: Truncated ^{1}H NMR titration spectra of rotaxane **9** upon addition of a)$LiClO_4$, b) NaBArF (500 MHz, 298 K, 7:3 $CDCl_3$:CD_3CN, [Rot.**9**] = 1.0 mM). (Connecting lines are to guide the eye only)*

S4. DFT calculations

DFT calculations were carried out in the gas phase using Gaussian 16[9] at the B3LYP level of theory[10] using aug-cc-pVTZ basis set for chlorine atoms, aug-cc-pVTZ-PP basis set for larger halide atoms, and 6-31g* basis for the other atoms.[11-13] Counterpoise correction was invoked to correct for basis set superposition error.[14, 15] Obtained crystal structures were used as starting coordinates. Terminal benzene moieties of the axles were replaced by methyl groups for the ease of simulation.

S4.1. DFT optimised structures

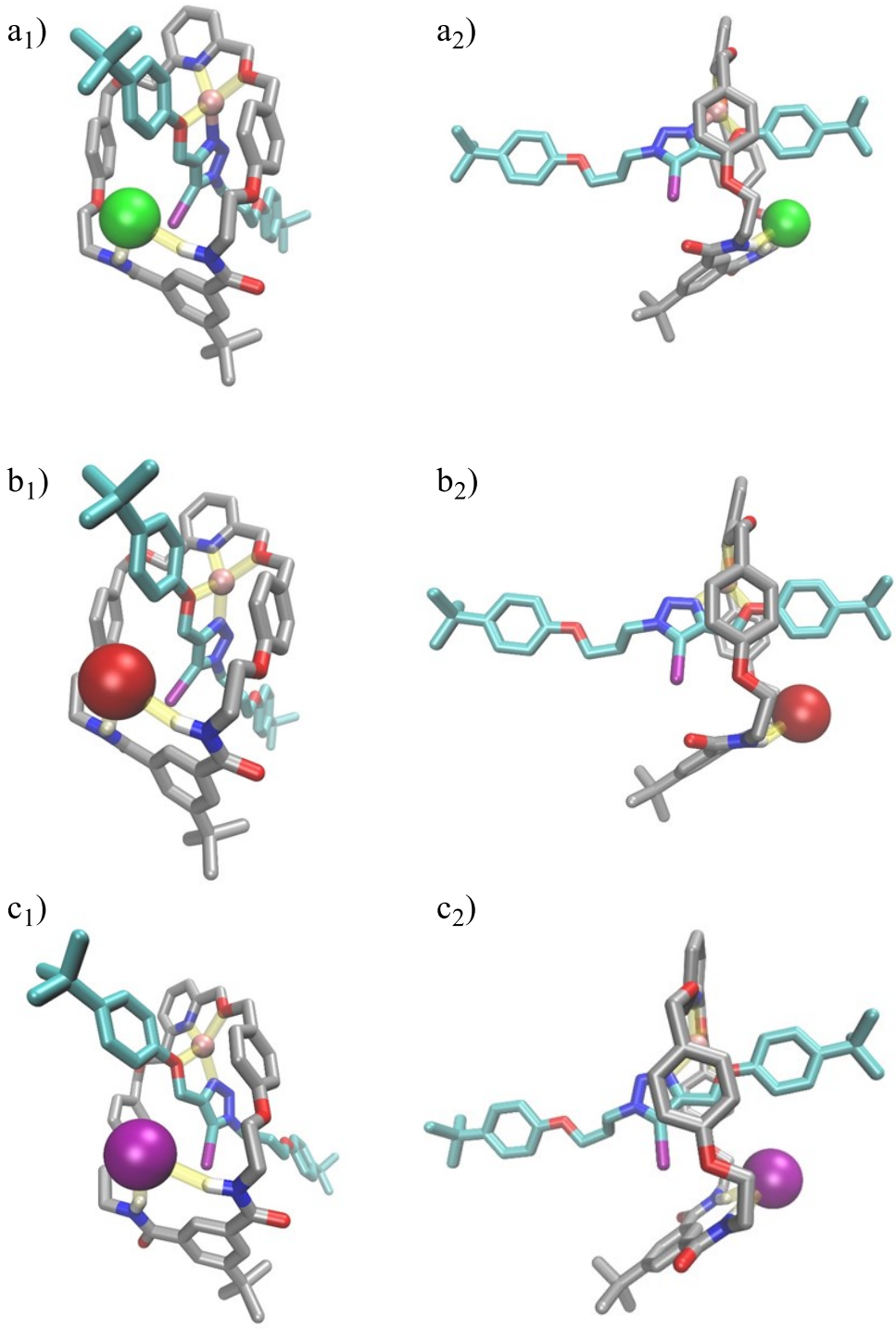

*Figure S4.1: DFT optimised ion-pair bound rotaxane **10**; a) LiCl bound rotaxane **10** (front and size view), b) LiBr bound rotaxane **10** (front and size view), c) LiI bound rotaxane **10** (front and size view), Colour code of atoms: O-red, N-blue, I-purple, Li-pink, Br- brown, Cl-green, $C_{(MC)}$ -gray $C_{(axle)}$-teal. Host-guest interactions are shown by yellow*

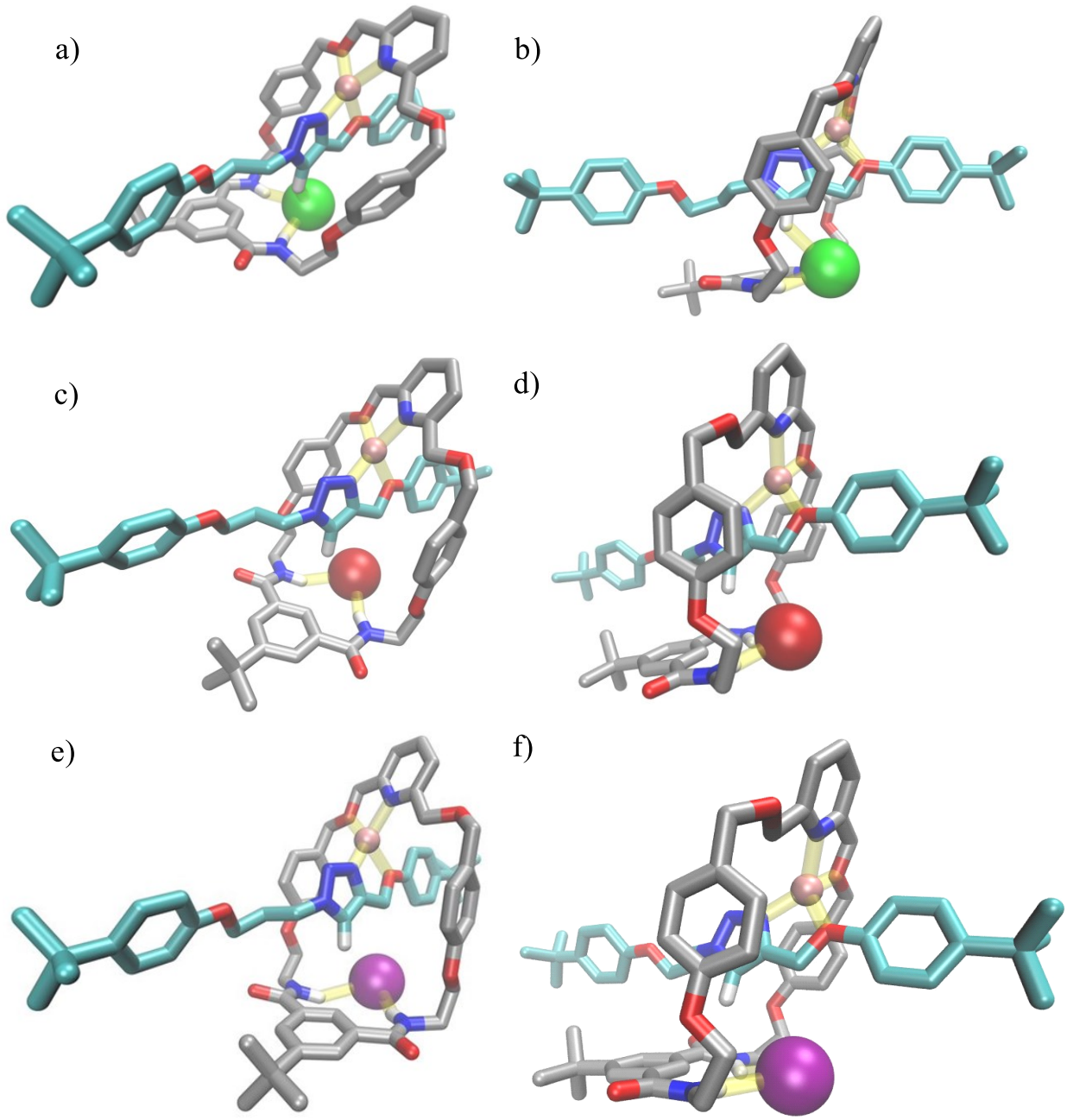

*Figure S4.2: DFT optimised ion-pair bound rotaxane **9**; a) front view of LiCl bound rotaxane **9**, b) side view of LiCl bound rotaxane **9**, c) front view of LiBr bound rotaxane **9**, d) side view of LiBr bound rotaxane **9**, e) front view of LiI bound rotaxane **9,** f) side view of LiI bound rotaxane **9.** Colour code of atoms: O-red, N-blue, I-purple, Li-pink, Br- brown, Cl-green, $C_{(MC)}$ -gray $C_{(axle)}$-teal. Host-guest interactions are shown by yellow. Based on the tabulated data in Table S4.1 an overlap of van der Waals and ionic radii were observed between triazole HB donor and Cl^-.*

Table S4.1: Calculated summation of van der Waals and ionic radii of H and halide anion and the observed distance between the triazole HB donor and the anion in the DFT optimised structure. [a]

	Calculated (Å)	Observed (Å)
H···Cl$^-$	3.01	2.83
H···Br$^-$	3.16	3.258
H···I$^-$	3.4	3.698

[a]*ionic and van der Waals radii were calculated using literature data.*[16, 17]

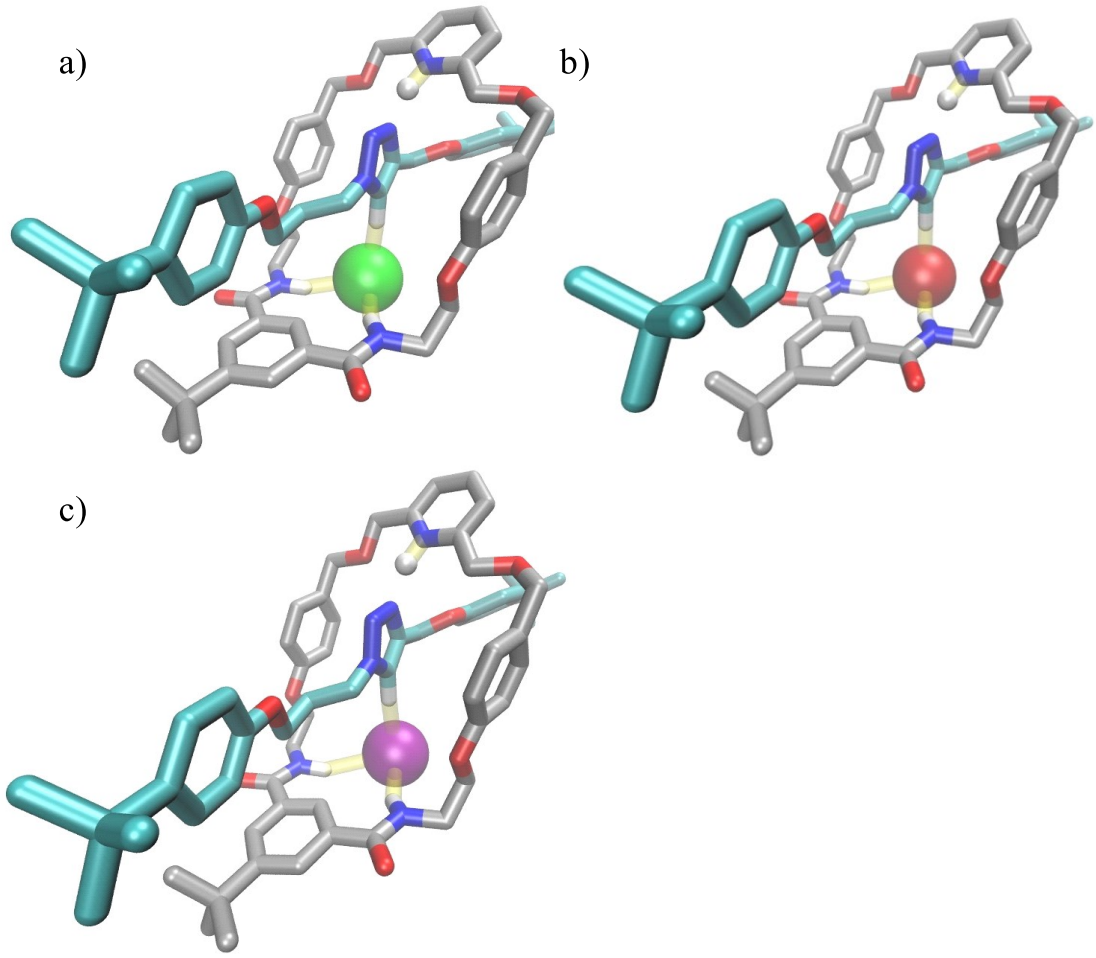

*Figure S4.3: DFT optimised ion-pair bound rotaxane **10**; a) HCl bound rotaxane **10**, b) HBr bound rotaxane **10**, c) HI bound rotaxane **10.** Colour code of atoms: H-white, O-red, N-blue, I-purple, Li-pink, Br- brown, Cl-green, $C_{(MC)}$ -gray $C_{(axle)}$-teal. Host-guest interactions are shown by yellow*

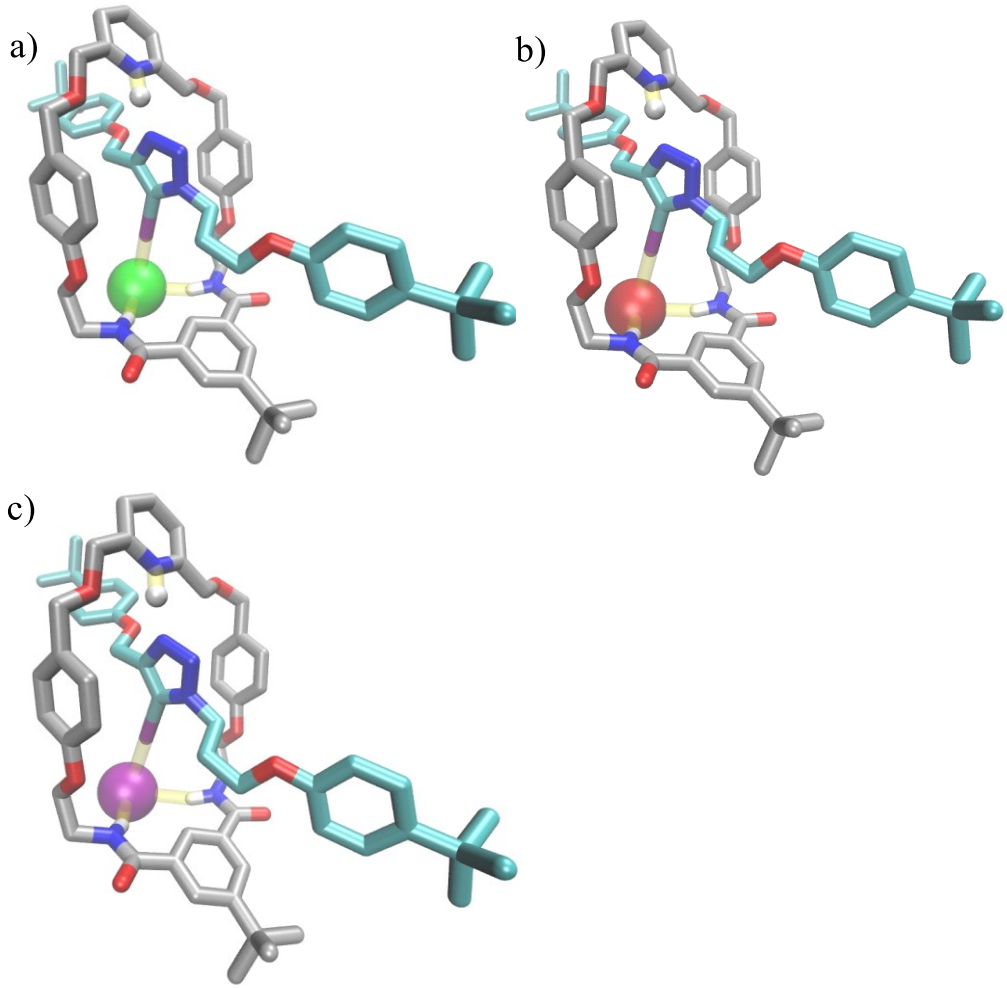

*Figure S4.4: DFT optimised ion-pair bound rotaxane **9**; a) HCl bound rotaxane **9**, b) HBr bound rotaxane **9**, c) HI bound rotaxane **9**, Colour code of atoms: H-white, O-red, N-blue, I-purple, Li-pink, Br- brown, Cl-green, $C_{(MC)}$ -gray $C_{(axle)}$-teal. Host-guest interactions are shown by yellow*

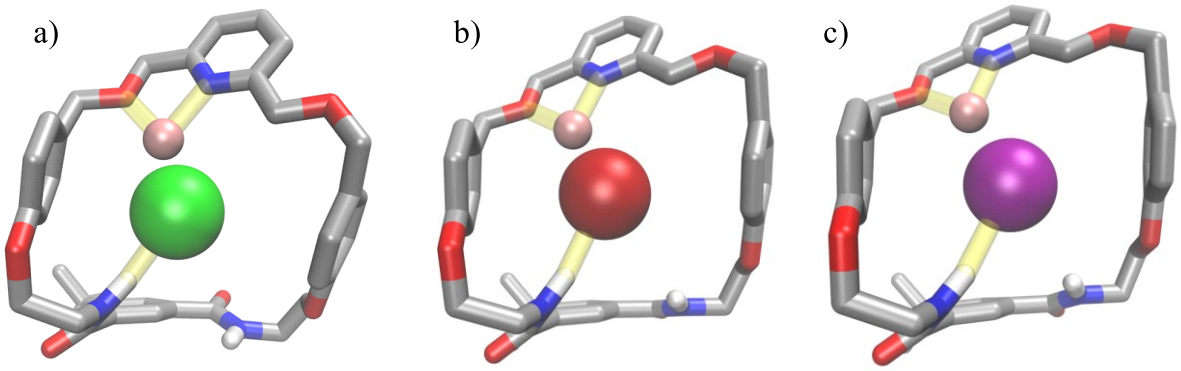

*Figure S4.5: DFT optimised ion-pair bound macrocycle **6**; a) LiCl bound macrocycle **6**, b) LiBr bound macrocycle **6**, c) LiI bound macrocycle **6**, Colour code of atoms: H-white, O-red, N-blue, I-purple, Li-pink, Br- brown, Cl-green, C-gray. Host-guest interactions are shown by yellow*

S4.2. Electrostatic potential map

It was postulated that the cation complexation to the rotaxane through the triazole nitrogen atom in the axle, could polarise the connecting HB/XB donor atoms. To this end, rotaxane **9** and **10** which have triazole HB and XB donors respectively in the axle were chosen to map the ESP surface to investigate the effect of Li^+/H^+ complexation towards the electrostatic potential of the HB/XB donor atoms.

Binding of Li^+ and H^+ increase the electrostatic potential of the axle HB donor of rotaxane **9** from 186 kcal/mol to 252 kcal/mol and 249 kcal/mol. A similar increase from 227 kcal/mol to 284 kcal/mol and 288 kcal/mol is observed for the axle XB donor of rotaxane **10**.

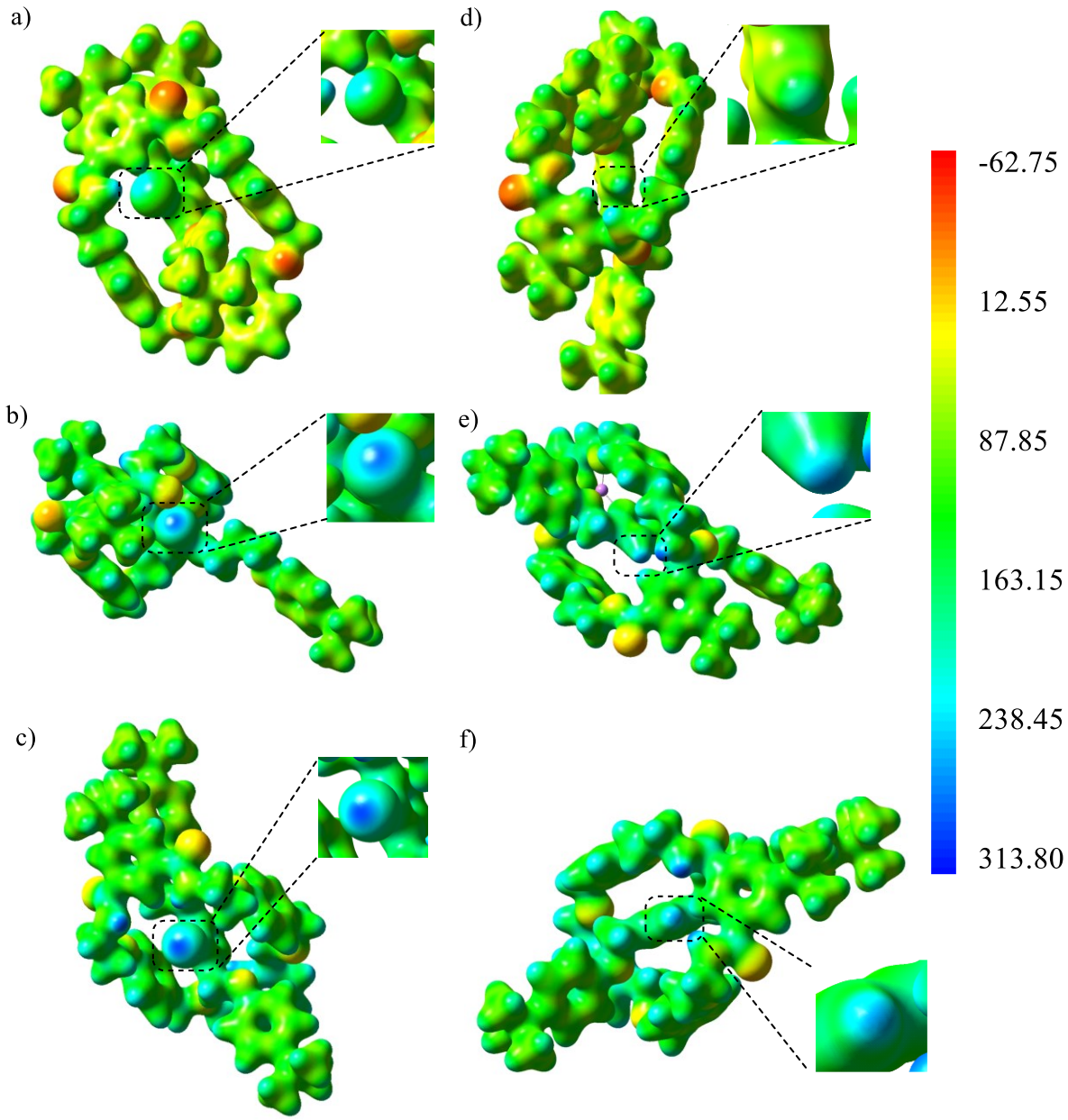

*Figure S4.6: Electrostatic potential maps of a) rotaxane **10**, b) Li^+ complexed rotaxane **10,** c) H^+ rotaxane **10**, d) rotaxane **9**, e) Li^+ complexed rotaxane **9**, f) H^+ rotaxane **9**. Triazole XB/HB donors of rotaxane **9** and **10** are magnified for clarity. Colour coded isosurface values are given in kcal/mol.*

S5. References

1. V. K. Munasinghe, J. Pancholi, D. Manawadu, Z. Zhang and P. D. Beer, *Chem. Eur. J.*, 2022, **28**, e202201209.
2. A. Brown, K. M. Mennie, O. Mason, N. G. White and P. D. Beer, *Dalton Trans.*, 2017, **46**, 13376-13385.
3. H. Zheng, W. Zhou, J. Lv, X. Yin, Y. Li, H. Liu and Y. Li, *Chem. Eur. J.*, 2009, **15**, 13253-13262.
4. N. L. Kilah, M. D. Wise, C. J. Serpell, A. L. Thompson, N. G. White, K. E. Christensen and P. D. Beer, *J. Am. Chem. Soc.*, 2010, **132**, 11893-11895.
5. V. Aucagne, K. D. Hänni, D. A. Leigh, P. J. Lusby and D. B. Walker, *J. Am. Chem. Soc.*, 2006, **128**, 2186-2187.
6. G. Sheldrick, *Acta Crystallographica Section A*, 2015, **71**, 3-8.
7. G. Sheldrick, *Acta Crystallographica Section C*, 2015, **71**, 3-8.
8. P. Thordarson, *Chem. Soc. Rev.*, 2011, **40**, 1305-1323.
9. M. J. Frisc, G. W. Trucks, H. B. Schlegel, G. E. Scuseria, M. A. Robb, J. R. Cheeseman, G. Scalmani, V. Barone, B. Mennucci, G. A. Petersson and others, *Gaussian Inc, Wallingford*.
10. A. D. Becke, *The Journal of Chemical Physics*, 1993, **98**, 5648-5652.
11. D. E. Woon and T. H. Dunning, Jr., *The Journal of Chemical Physics*, 1993, **98**, 1358-1371.
12. K. A. Peterson, B. C. Shepler, D. Figgen and H. Stoll, *The Journal of Physical Chemistry A*, 2006, **110**, 13877-13883.
13. K. A. Peterson, D. Figgen, E. Goll, H. Stoll and M. Dolg, *The Journal of Chemical Physics*, 2003, **119**, 11113-11123.
14. S. F. Boys and F. Bernardi, *Mol. Phys.*, 1970, **19**, 553-566.
15. F. B. van Duijneveldt, J. G. C. M. van Duijneveldt-van de Rijdt and J. H. van Lenthe, *Chem. Rev.*, 1994, **94**, 1873-1885.
16. R. Shannon, *Acta Crystallographica Section A*, 1976, **32**, 751-767.
17. S. Alvarez, *Dalton Trans.*, 2013, **42**, 8617-8636.